



ELSEVIER

Contents lists available at ScienceDirect

Environment International

journal homepage: www.elsevier.com/locate/envint

Impact of biochar on mobilization, methylation, and ethylation of mercury under dynamic redox conditions in a contaminated floodplain soil

Felix Beckers^a, Yasser Mahmoud Awad^{a,b,c}, Jingzi Beiyan^{a,d,e}, Jens Abrigata^a, Sibylle Mothes^f, Daniel C.W. Tsang^e, Yong Sik Ok^{b,*}, Jörg Rinklebe^{a,g,**}

^a University of Wuppertal, Institute of Foundation Engineering, Waste and Water Management, School of Architecture and Civil Engineering, Soil and Groundwater Management, Pauluskirchstraße 7, 42285 Wuppertal, Germany

^b Korea Biochar Research Center, O-Jeong Eco-Resilience Institute (OJERI) & Division of Environmental Science and Ecological Engineering, Korea University, Seoul 02841, Republic of Korea

^c Faculty of Agriculture, Suez Canal University, Ismailia 41522, Egypt

^d School of Environment and Chemical Engineering, Foshan University, Foshan, Guangdong, China

^e Department of Civil and Environmental Engineering, The Hong Kong Polytechnic University, Hung Hom, Kowloon, Hong Kong, China

^f UFZ Helmholtz Centre for Environmental Research, Department of Analytical Chemistry, Permoserstraße 15, 04318 Leipzig, Germany

^g Department of Environment, Energy & Geoinformatics, Sejong University, 98 Gunja-Dong, Guangjin-Gu, Seoul, Republic of Korea

ARTICLE INFO

Keywords:

Mercury
Redox processes
Wetlands
Biochar
Agro-environmental management
PLFA

ABSTRACT

Mercury (Hg) is a highly toxic element, which is frequently enriched in flooded soils due to its anthropogenic release. The mobilization of Hg and its species is of ultimate importance since it controls the transfer into the groundwater and plants and finally ends in the food chain, which has large implications on human health. Therefore, the remediation of those contaminated sites is an urgent need to protect humans and the environment. Often, the stabilization of Hg using amendments is a reliable option and biochar is considered a candidate to fulfill this purpose. We tested two different pine cone biochars pyrolyzed at 200 °C or 500 °C, respectively, with a view to decrease the mobilization of total Hg (Hg_t), methylmercury (MeHg), and ethylmercury (EtHg) and/or the formation of MeHg and EtHg in a contaminated floodplain soil (Hg_t: 41 mg/kg). We used a highly sophisticated automated biogeochemical microcosm setup to systematically alter the redox conditions from ~ -150 to 300 mV. We continuously monitored the redox potential (E_H) along with pH and determined dissolved organic carbon (DOC), SUVA₂₅₄, chloride (Cl⁻), sulfate (SO₄²⁻), iron (Fe), and manganese (Mn) to be able to explain the mobilization of Hg and its species.

However, the impact of biochar addition on Hg mobilization was limited. We did not observe a significant decrease of Hg_t, MeHg, and EtHg concentrations after treating the soil with the different biochars, presumably because potential binding sites for Hg were occupied by other ions and/or blocked by biofilm. Solubilization of Hg bound to DOC upon flooding of the soils might have occurred which could be an indirect impact of E_H on Hg mobilization. Nevertheless, Hg_t, MeHg, and EtHg in the slurry fluctuated between 0.9 and 52.0 µg/l, 11.1 to 406.0 ng/l, and 2.3 to 20.8 ng/l, respectively, under dynamic redox conditions. Total Hg concentrations were inversely related to the E_H; however, ethylation of Hg was favored at an E_H around 0 mV while methylation was enhanced between -50 and 100 mV. Phospholipid fatty acid profiles suggest that sulfate-reducing bacteria may have been the principal methylators in our experiment. In future, various biochars should be tested to evaluate their potential in decreasing the mobilization of Hg and to impede the formation of MeHg and EtHg under dynamic redox conditions in frequently flooded soils.

1. Introduction

Soil contamination with mercury (Hg) is a challenging issue for

human and environmental health since Hg and its species are particularly toxic (Pushie et al., 2014; Tipping et al., 2010). Toxicity and mobility are determined by its chemical speciation as influenced by the

* Corresponding author.

** Correspondence to: J. Rinklebe, University of Wuppertal, Institute of Foundation Engineering, Waste and Water Management, School of Architecture and Civil Engineering, Soil and Groundwater Management, Pauluskirchstraße 7, 42285 Wuppertal, Germany.

E-mail addresses: yongsikok@korea.ac.kr (Y.S. Ok), rinklebe@uni-wuppertal.de (J. Rinklebe).

<https://doi.org/10.1016/j.envint.2019.03.040>

Received 19 December 2018; Received in revised form 14 March 2019; Accepted 14 March 2019

Available online 02 April 2019

0160-4120/© 2019 Published by Elsevier Ltd. This is an open access article under the CC BY-NC-ND license

(<http://creativecommons.org/licenses/by-nc-nd/4.0/>).

environmental conditions. It has been shown that the highly toxic species methylmercury (MeHg; CH_3Hg^+) occurs naturally where environmental conditions favor the net methylation of Hg while its industrial use was limited to some fungicides (Bakir et al., 1973; Beckers and Rinklebe, 2017; Hunter et al., 1940). Consequently, greater knowledge on conditions favoring Hg methylation and methods to impede its formation are needed. It is known that Hg methylation is primarily performed by anaerobic sulfate-reducing bacteria (SRB) (Janssen et al., 2016; Parks et al., 2013). Furthermore, it was found that MeHg concentrations in a flooded soil were particularly high at redox potentials ($E_{\text{H}_2\text{S}}$) that fall within the range of sulfate reduction (unpublished data). Additionally, materials have to be found that are suitable to immobilize MeHg and the second important organic Hg species ethylmercury (EtHg; $\text{CH}_3\text{CH}_2\text{Hg}^+$) in soil. Ethylmercury has been identified in soil samples and it has been suggested that it may exist widely in the environment (Mao et al., 2010). However, information on microbial formation of EtHg is lacking (Hintelmann, 2010), and little is known on other formation pathways and its behavior in natural environments due to analytical limitations (Kodamatani and Tomiyasu, 2013; Lusilao-Makiiese et al., 2016; Mao et al., 2010). Floodplain soils occupy a critical position among Hg polluted soils as they are subject to periodic inundations which can promote low redox conditions, Hg methylation and mobilization of Hg species (Beckers and Rinklebe, 2017). Particularly organic-rich floodplain soils have been identified as Hg methylation sites and sources for enhanced MeHg contribution to adjacent streams (Devai et al., 2005; Lázaro et al., 2016; Roulet et al., 2001).

Ways to either remove Hg or to efficiently immobilize it by transforming it into its most stable and least toxic forms in situ are required (Cassina et al., 2012; Ullah et al., 2015; Wang et al., 2013; Xu et al., 2015). The utilization of soil amendments is one possible remediation technique to diminish Hg mobility in soil (Shu et al., 2016a; Šípková et al., 2016; Zhu et al., 2015). Among these amendments biochar seems promising owing to its positive properties: Its production from organic waste materials is cost-efficient and it may fertilize the soil while simultaneously immobilizing Hg species (Shu et al., 2016a). Biochar is a carbon-rich material which is produced via pyrolysis of agricultural bio-waste such as wood chips, crop straw or vegetable waste under oxygen limitation (Ahmad et al., 2017; Ahmad et al., 2014; Igalavithana et al., 2017). Its potential to remove Hg from solution (Kong et al., 2011; Xu et al., 2016) and combustion flue gas (Klasson et al., 2014; Shen et al., 2017; Tan et al., 2011; Yang et al., 2016), and to reduce the MeHg levels in rice grains (Shu et al., 2016b), or to immobilize MeHg in soil (Shu et al., 2016a) has already been demonstrated. Still, different feedstocks, pyrolysis temperatures, and functionalizations warrant examination to identify additional biochars with high Hg sorption potential (Park et al., 2019; Xia et al., 2019; Zhang et al., 2019).

Therefore, our objectives were (i) to examine the impact of pre-defined redox conditions on the release dynamics of dissolved Hg_t , MeHg, and EtHg in a contaminated floodplain soil treated with biochar pyrolyzed either at 200 °C (BC200) or 500 °C (BC500), and non-treated (control), (ii) to identify the underlying redox-driven processes mechanistically with particular emphasis on parameters which are thought to affect Hg methylation, (iii) to quantify the efficiency of both biochars as immobilizing agents to reduce the concentrations of Hg_t , MeHg, and EtHg in soil solution, and (iv) to determine the relationship between shifts in Hg species and alterations in the soil microbial community structure as identified by phospholipid fatty acid (PLFA) analysis.

2. Materials and methods

2.1. Soil sampling and characterization

The sampling site is located in North Rhine-Westphalia, Germany, in a Hg-polluted Wupper River floodplain close to the Wupperinsel nature reserve at the lower course of the river (2568987 E, 5659539 N;

51°4′0.449″N, 6°59′0.718″E). The floodplain is periodically inundated, typically in spring, and cultivated as grassland. A soil profile within the floodplain was excavated before and described in detail (Frohne and Rinklebe, 2013). The soil was classified as Eutric Fluvisol according to IUSS (2015). The Hg_t content of the soil horizon within 26 to 40 cm was 41.0 mg/kg, which substantially exceeds the applicable action value (2 mg/kg) of the German Federal Soil Protection and Contaminated Sites Ordinance in relation to plant quality for the soil – plant transfer of metals on grasslands (BBodSchV, 1999). Therefore, soil material was collected from this depth from a 4 m² area and homogenized in one composite sample.

Soil properties were determined following standard methods described in Blume et al. (2011). Soil pH was measured according to DIN EN 15933 (2012). Pseudo total metal concentrations within subsamples of CS, BC200, and BC500 were measured by inductively coupled plasma optical emission spectrometry (ICP-OES) (Ultima 2, Horiba Jobin Yvon, Unterhaching, Germany) after subsample digestion in a microwave system (MLS 1200 Mega, MLS GmbH, Leutkirch, Germany) following U.S. EPA Method 3051A (2007). Total Hg was determined with atomic absorption spectrometry (AAS) using a DMA-80 direct mercury analyzer (MLS GmbH, Leutkirch, Germany). The Hg species MeHg and EtHg were analyzed using gas chromatography with atomic emission detection (GC-AED) (HP 6890, Agilent, Waldbronn, Germany - jas 2350, jas GmbH, Moers, Germany). Sample aliquots were adjusted to pH 4.5–5 by addition of an acetic/acetate buffer and sodium tetrapropylborate for derivatization. More detailed information on the analytical procedures is provided in the Supporting Information.

2.2. Biochar production

Fallen pine cones were collected at the Kangwon National University, Chuncheon, South Korea, and dried in a greenhouse before biochar production. The dried pine cones were ground and sieved through a 2 mm sieve. Biochar production was carried out by a heating program in a muffle furnace (LT, Nabertherm, Lilienthal, Germany) under limited supply of air. The heating rate was 7 °C/min, and the holding time at the desired temperature (200 °C or 500 °C) was 2 h. The biochar was cooled down to 30 °C inside the muffle furnace (Igalavithana et al., 2017). By this, two biochars were produced, pyrolyzed either at 200 °C (BC200) or 500 °C (BC500).

2.3. Soil and biochar characteristics and soil incubation

Major properties of the soil and the used amendments BC200 and BC500 are given in Table 1. Silt constituted the main fraction of soil texture and the soil was found to be slightly acidic (pH 6.4). The soil had a high organic carbon content (7.1%) and a high content of Hg_t (31.2 ppm). The high Hg content can be attributed to discharges from metal industries such as electroplating, the production and use of Hg-containing fungicides, the production of Hg thermometers, and the textile industry, particularly from dye factories, during the last centuries in the proximity of the river leading to the contamination of the water, the sediments, and the floodplains of the Wupper River (Frohne and Rinklebe, 2013; Frohne et al., 2012; Schenk, 1994). Soil MeHg content (0.44 mg/kg) was very high. In contrast, the EtHg content (0.10 µg/kg) was slightly lower than levels reported from the Florida Everglades (Cai et al., 1997; Mao et al., 2010).

Two subsamples of the contaminated Wupper soil were amended with either BC200 or BC500. Both, BC200 and BC500 were applied to the subsamples at a rate of 80 t/ha. The soil and the amendments were mixed thoroughly, subsequently maintained at 70% water holding capacity and incubated at 25 °C for 40 days. After incubation, the soil was air-dried and subsequently used for the redox experiment.

Table 1

Properties and element concentrations (microwave digestion) of the contaminated soil (CS), as well as properties of the biochars BC200 and BC500.

Soil	Sand	Silt	Clay	Total carbon	Total organic carbon	Total nitrogen	Total carbonates	pH ^a	Hg _t	Fe	Mn	Al	S
	%	%	%	%	%	%	%		[mg/kg]	[g/kg]	[g/kg]	[g/kg]	[g/kg]
Wupper (CS)	6	92	2	7.06	7.05	0.35	0.04	6.4	31.19	43.8	0.87	18.5	0.99

Biomass	Pyrolysis temperature	Biochar	Mobile matter	Ash	Resident matter	C ^b	H ^b	N ^b	O ^b	H/C	O/C	pH ^c	Hg _t	EC ^c	Surface area ^d	APV ^e	APD ^e
	°C		%	%	%	%	%	%	%				[mg/kg]	dS/m	m ² /g	× 10 ⁻³ m ³ /g	nm
Pine cone	200	BC200	62.35	0.77	35.6	69.74	2.13	1.03	27.09	0.42	0.21	4.15	0.026	0.001	0.47	2.38	45.13
	500	BC500	10.01	8.96	79.6	74.64	2.62	1.81	20.94	0.37	0.29	6.77	0.007	0.001	192.97	10.2	2.44

APV, average pore volume; APD, average pore diameter.

^a pH determined according to DIN EN 15933 (2012) [H₂O].^b Moisture and ash free.^c 1:20 ratio of biochar to deionized water.^d Brunauer-Emmett-Teller (BTE) method.^e Barret-Joyner-Halender (BJH) method.

2.4. Experiment under pre-set redox conditions

The impact of dynamic redox conditions on the mobilization of Hg_t, MeHg, and EtHg was determined using an automated biogeochemical microcosm system in the laboratory. Flooding of the contaminated soil (CS), contaminated soil + Biochar 200 (CS + BC200), and contaminated soil + Biochar 500 (CS + BC500) was simulated in the microcosms (MCs). We worked with four MCs per amendment treatment to take into account the natural soil heterogeneity. Thus, twelve biogeochemical microcosms were used in total.

The biogeochemical microcosm system enables the user to set and maintain pre-defined redox windows by automatically flushing the slurry, obtained by continuous stirring of the flooded soil, with oxygen (O₂) or nitrogen (N₂) when the E_H falls below or exceeds pre-set E_H values. The system has been utilized in several studies (e.g. Beiyuan et al., 2017). Nine redox windows were set in line with this experiment covering the range between ~ -150 to 300 mV. Thus, using the redox condition ranges classified by Bohn (1971) where the E_H range 100 to 400 mV = moderately reduced soils; between -100 and 100 mV = reduced soils; and -100 to -300 mV = highly reduced soils, redox conditions in the course of the experiment were changed stepwise from highly reducing conditions to moderately reducing conditions. The E_H was maintained for approximately 24 h within each pre-defined redox window before sampling. Collected samples were separated in a liquid and a solid phase by 0.45 μm filtration. Subsamples were analyzed for Hg_t, MeHg, EtHg, dissolved organic carbon (DOC), chloride (Cl⁻), iron (Fe), manganese (Mn), sulfur (S), sulfate (SO₄²⁻), and PLFA, while ultraviolet (UV) absorbance at λ = 254 nm was determined to calculate specific UV absorbance at 254 nm (SUVA₂₅₄). Detailed experiment specific information is provided in Supporting Information while further technical information on the automated biogeochemical microcosm system was compiled by Yu and Rinklebe (2011).

2.5. Phospholipid fatty acid analysis

Phospholipid fatty acid analysis was used to assess the microbial community in the solid material obtained by filtration of the collected samples. In particular, changes in the SRB community were of interest. Phospholipid extraction and PLFA analysis were performed on 2 g of frozen solid material using the procedure described by White et al. (1979) and Frostegård et al. (1991). The PLFAs were designated following the nomenclature described by Feng et al. (2003). Detailed information on which PLFAs were considered to identify the SRB community and further detailed experimental information is provided in the Supporting Information.

2.6. Calculations and statistical analysis

Redox potential and pH values were automatically recorded by a data logger on 10 min intervals. This dataset was used to calculate the mean values of E_H and pH levels for 3, 6, 12, and 24 h prior to sampling. Correlation analyses were performed between these E_H/pH values and the mean concentrations of Hg_t, MeHg, EtHg, DOC, SO₄²⁻, Fe, and Mn, which were computed by dividing the sum of analysis results for the individual replications by the number of MCs used per type of soil. The closest correlations were found for the E_H/pH results 6 h before sampling which were therefore used for statistics. The programs IBM SPSS Statistics 25 and GraphPad Prism 5 were used for descriptive statistics. SPSS 25 was used for calculating correlations and performing of principal component factor analyses. The latter were carried out using the varimax rotation procedure to make components easier to interpret. Component plots in rotated space were used to provide a visual representation of factor analyses loadings plotted in a 2-dimensional space.

3. Results and discussion

3.1. Soil E_H and pH

The observed E_H values (E_H all) in the slurries of CS and the biochar treatments (CS + BC200 and CS + BC500) fell within the range of highly reduced and moderately reduced conditions (Table 2, Fig. 1). The pH (pH all) values in the slurries varied between very strongly acidic to neutral (CS and CS + BC500) and slightly alkaline (CS + BC200) (Table 2). The pH in the slurry of CS and the biochar treatments showed an opposite behavior to E_H (Fig. 1). Therefore, the correlation between soil E_H and pH was negative for the overall trends ($r = -0.68$; $p < 0.01$; $n = 11,856$ in CS; $r = -0.72$; $p < 0.01$; $n = 11,910$ in CS + BC200; and $r = -0.79$; $p < 0.01$; $n = 11,353$ in CS + BC500; data not shown) as well as for the data collected when the microcosms were sampled ($r = -0.70$; $p < 0.00001$; $n = 36$ in CS, $r = -0.77$; $p < 0.00001$; $n = 36$ in CS + BC200, and $r = -0.85$; $p < 0.00001$; $n = 36$ in CS + BC500).

The inverse relationship of pH and E_H was expected, presumably due to the consumption of protons required for the reduction of NO₃⁻, Mn⁴⁺, Fe³⁺, and SO₄²⁻ (Reddy and DeLaune, 2008; Yu et al., 2007). The results indicate that the application of both BC200 and BC500 to CS exerted no significant influence on the pH in soil slurry, with only a slightly lower pH found in CS + BC500 (Table 2).

Table 2

Redox potential (E_H), pH, concentrations of MeHg and EtHg in the slurry, as well as concentrations of Hg_t and other elements/compounds in the slurry filtrate of the contaminated soil (CS), the contaminated soil plus Biochar 200 (CS + BC200), and the contaminated soil plus Biochar 500 (CS + BC500) during the experiment.

Parameter	Unit	Contaminated soil				Contaminated soil + Biochar 200				Contaminated soil + Biochar 500			
		N	Minimum	Maximum	Mean	N	Minimum	Maximum	Mean	N	Minimum	Maximum	Mean
E_H all	[mV]	11,856	-126	299	86	11,910	-150	307	80	11,575	-119	302	90
E_H^a		36	-113	296	75	36	-132	299	74	34	-118	296	82
pH all		11,860	4.9	7.0	5.8	11,915	4.8	7.5	5.8	11,415	4.5	6.9	5.6
pH ^a		36	4.9	6.9	5.7	36	4.8	6.6	5.7	34	4.5	6.6	5.5
Hg_t	[μ g/l]	36	1.8	52.0	13.0	36	1.0	51.8	11.9	34	0.9	35.3	10.0
MeHg	[ng/l]	35	21.3	406.0	87.7	36	11.1	392.0	80.4	34	11.2	210.0	75.5
EtHg		33	3.1	17.1	7.4	34	2.3	17.9	6.9	32	2.8	20.8	7.0
DOC	[g/l]	36	1.33	2.80	2.31	36	1.66	2.82	2.33	34	1.31	2.84	2.14
SUVA ₂₅₄	[l/mg C/m]	36	0.07	0.12	0.09	36	0.07	0.19	0.10	34	0.07	0.31	0.11
Cl ⁻	[mg/l]	36	50.0	156.3	91.5	36	46.5	157.6	88.0	34	55.1	172.7	98.4
SO ₄ ²⁻		36	25.6	76.9	33.4	35	23.8	94.2	37.5	34	23.9	63.9	35.2
Fe		36	0.6	106.9	9.5	36	0.5	183.9	10.2	34	0.4	187.7	18.7
Mn		36	5.7	73.6	30.9	36	7.0	76.1	25.3	34	6.7	70.6	34.5

DOC: dissolved organic carbon.

N: number of samplings/measurements.

^a Means of data 6 h before sampling.

3.2. Impact of E_H /pH changes on mobilization of Hg_t , MeHg, and EtHg in CS, CS + BC200, and CS + BC500

3.2.1. Impact of E_H /pH changes on mobilization of Hg_t in CS, CS + BC200, and CS + BC500

The mobilization of Hg_t in the CS was particularly high under low redox conditions (Fig. 2). Hence, the highest concentrations of dissolved Hg_t were determined for the first two samplings at E_H -92 mV (29 μ g/l) and -110 mV (28 μ g/l).

The high mean concentration found for the second sampling at E_H -110 mV was significantly affected by one of the four CS MCs in which the Hg_t concentration increased up to 52 μ g/l. The average 6 h E_H value for this MC was slightly lower (4–5 mV) compared to the other MCs in which Hg_t declined even though E_H values were lower than during the first sampling. Here, the pH may have had an effect: The pH value of the MC (6.9) was higher than in the other MCs (6.5; 6.3; 6.3). Mercuric mercury (Hg(II)) shows a different behavior than most other divalent metals as its extent of adsorption is greatest in acidic media (Barrow and Cox, 1992; Pelcová et al., 2010; Sarkar et al., 1999; Yin et al., 1996). The close link between Hg_t dissolution and pH in CS is supported by a significant positive correlation (Table 3).

However, it is unlikely that the pH was the main influencing factor. Xu et al. (2014) observed enhanced Hg desorption at pH 5 and 11 but generally found that pH adjustment was insufficient for Hg removal since only $\leq 0.3\%$ of soil Hg_t was mobilized at these pH values in their soil washing experiments. In our study, the relationship between Hg_t and E_H in CS was also strong. We found an inverse relationship with decreasing Hg_t concentrations when E_H increased. Correspondingly, Hg_t concentrations were found to be higher at the last two samplings when E_H had been lowered again (Fig. 2, Table 3). Moreover, the lowest mean Hg_t concentration (3 μ g/l) was determined for the highest mean E_H (282 mV).

In general, the pattern of Hg_t concentrations found in CS + BC200 and CS + BC500 was similar to the one observed in CS. However, under highly reduced conditions, at the second sampling, Hg_t concentrations were considerably lower in both biochar treatments (Fig. 2): The mean Hg_t concentration in CS was as high as 28 μ g/l while those calculated for CS + BC200 (16 μ g/l) and CS + BC500 (14 μ g/l) constituted about half of the CS value. Even when excluding the MC with the highest Hg_t concentrations in CS the difference would be at least 4.7 μ g/l. This is noteworthy since the pattern of Hg_t concentrations in CS and the biochar treatments differed by no > 2.3 μ g/l from E_H window 0 mV on. Moreover, the mean Hg_t concentration for all measurements was similar in CS, CS + BC200, and CS + BC500 (Table 2). To our knowledge

there is no information available on changing abilities of biochars to sorb inorganic Hg at varying redox conditions. However, Xu et al. (2016) revealed that different biochars may sorb Hg via different complexation mechanisms. They found that Hg sorption by bagasse (crushed sugarcane stalks) biochar produced at 450 °C was primarily attributed to the formation of $(-COO)_2Hg$ and $(-O)_2Hg$ while hickory chip biochar produced at the same temperature sorbed Hg by the π electrons of C=C and C=O induced Hg- π binding. Liu et al. (2016) noted that Hg removal mechanisms by carbonaceous sorbents include coordination between Hg and functional groups on/within sorbents, reduction of Hg(II) to Hg(I) and precipitation, and co-precipitation with anions. However, they concluded that the chemical binding of Hg to functional groups such as thiol, hydroxyl, carboxylic and chloride on the surface of and within biochars appears to be the predominant removal mechanism. Furthermore, it was found that Hg was bound to S in biochars with high S contents and to O and Cl in biochars with low S contents (Liu et al., 2016). Dong et al. (2013) found that 23 to 31% of Hg sorbed by pepper biochars pyrolyzed at 300 °C and 450 °C was associated with carboxylic and 77 to 69% with phenolic hydroxyl groups. Contrarily, 91% of the Hg sorbed by pepper biochar pyrolyzed at 600 °C was associated with a graphite-like domain on an aromatic structure, with the rest associated with phenolic hydroxyl groups. The loss of functional groups with increasing temperature due to decreasing H and O resulted in a lower Hg sorption capacity, indicating that low pyrolysis temperature was beneficial to the production of biochars with higher Hg sorption potential (Dong et al., 2013). These results are in agreement with Klüpfel et al. (2014) who found that the pool of redox-active moieties was dominated by electron-donating, phenolic moieties at the pyrolysis temperatures 200 and 300 °C, by newly formed electron accepting quinone moieties at the pyrolysis temperatures 400 and 500 °C, and by electron accepting quinones and probably condensed aromatics at the pyrolysis temperatures 600 and 700 °C. Thus, we suggest that BC200 and BC500 had different moieties due to their distinct pyrolysis temperatures. However, the Hg_t immobilization potentials of BC200 and BC500 were marginal. Compared to CS mean Hg_t concentrations BC200 and BC500 reduced Hg_t release by 8% and 23%, respectively. The biochars primarily reduced Hg_t mobilization under highly reduced conditions around E_H -110 mV, at one specific sampling. Based on the chemistry of Hg interactions with DOC and other organic and inorganic soil components as well as on published results concerning Hg removal from aqueous solutions by means of biochar (Liu et al., 2018) we originally hypothesized that Hg would be immobilized more efficiently by BC200 and BC500. There are several possibilities why the amendment of BC200 and BC500 was not that effective in our experiment:

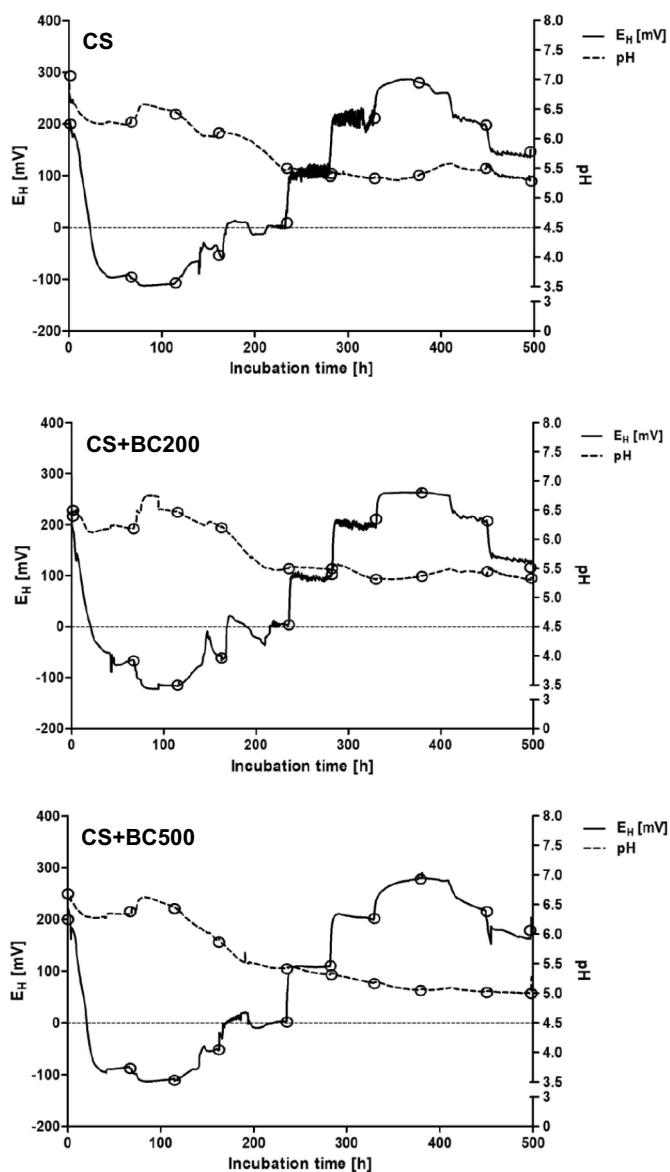


Fig. 1. Development of redox potential E_H (solid line), pH (dashed line), and sampling points (circles) in soil slurry (data every 10 min, averages were reported for an underlying dataset ($n \approx 11,915$) of four replicate samples) in the microcosms of untreated contaminated soil (CS), and soils treated with biochar pyrolyzed at 200 °C (CS + BC200), and biochar pyrolyzed at 500 °C (CS + BC500).

Typically, reduced sulfur groups are in great excess to Hg_t content in soils (Skylberg, 2012). Thus, the majority of Hg will bind to OM and metal sulfides while oxygen functional groups at Fe and Al oxyhydroxides as well as the edges of phyllosilicates are indirect adsorbents (Skylberg, 2012; Xia et al., 1999). Mercury in soil solution may be in the form of Hg^{2+} , $HgCl^+$, $HgCl_2^0$, $HgCl_3^-$, $HgCl_4^{2-}$, $HgClOH$, $Hg(OH)^+$, $Hg(OH)_2^0$, and $Hg-DOC$ (Han, 2007). However, due to its affinity for reduced sulfur groups, complexes with thiols from DOC will dominate the speciation of Hg in soil solution (Skylberg, 2012). Dissolved Hg concentrations measured in the course of our experiment exceeded those typically reported for natural ecosystems (Leopold et al., 2010). Therefore, it seems likely that Hg was not solely bound to the small fraction of DOC reactive thiol functional groups but also to carboxylic functional groups. Findings of Haitzer et al. (2002) indicated that the binding of Hg to DOM under natural conditions (very low Hg/DOM ratios) is controlled by a small fraction of DOM molecules

containing a reactive thiol functional group providing strong binding sites for Hg while carboxyl groups came into play at higher Hg to DOM ratios. It is noted that pH may influence the dissociation rate of carboxylic acids and thereby the number of potential binding sites.

Due to the strong binding between Hg and the reduced sulfur groups, the mobilization of Hg may be rather influenced more by DOC than by pH (Wallschläger et al., 1996; Xu et al., 2014). Besides protons, other cations such as Al^{3+} may occupy biochar binding sites. Another hypothesis why biochar showed little effect on Hg sorption is the presence of dissolved complexes binding Hg and hampering the sorption to biochar. Another factor which may affect Hg adsorption in the soil environment is the formation of biofilms. They may have formed in the course of the experiment as in nature cells grow predominantly in such aggregation of soil microorganisms, especially in heavily polluted sites (Gross et al., 2007). Thus, the alteration of the biochar surface and its chemical and physical properties by the formation of biofilms on the biochar particles needs to be considered. Possibly, biofilms may reduce the interaction of Hg with the biochar surface and thereby disturb its effects on Hg immobilization. Otherwise, biofilms themselves accumulate inorganic and methylated Hg compounds (Dranguet et al., 2017; Dranguet et al., 2018; Hintelmann et al., 1993) and may also lead to a higher rate of Hg methylation compared to planktonic bacteria (Lin et al., 2013). Different mechanisms play a role in Hg uptake by biofilms, e.g. steric hindrance and electrostatic interactions, binding functional groups of the extracellular polymeric substance matrix, and adsorption by mineral fractions present in biofilms (Dranguet et al., 2017). Leclerc et al. (2015) hypothesized that Hg-thiol complexation in the extracellular fractions of biofilms can occur which may potentially affect the bioavailability of Hg and increase its methylation.

The sorption of Hg-DOC complexes at the biochars was potentially of importance as we found strong positive relations between Hg_t and DOC (Table 3). Considering possible interactions between Hg-DOC complexes and BC200 as well as BC500 it has to be noted that Hg_t and DOC concentrations were only slightly lower in CS + BC500 (Table 2). Although often used for remediation purposes biochar amendments have been shown to have the potential to increase DOC concentrations, which may be linked to enhanced mobilization of soil contaminants (Beesley et al., 2010; Chen et al., 2018; Qi et al., 2017). In contrast, it has also been reported that DOC may readily sorb to biochar (Kammann et al., 2015). However, biochar mediated changes in DOC concentration may not always be detected (Jones et al., 2012). In general, the feedstock material and pyrolysis temperature influence properties of biochars, including their potential to release DOC (Liu et al., 2015). Here, minor effects of biochar amendment on DOC concentrations were observed.

The Hg sorption capacity of both biochars mainly came into effect under highly reduced conditions. One possible reason might be the cleavage of existing disulfide bonds of redox-active disulfides when they are reduced and the concomitant formation of vicinal thiol pairs which may bind Hg (Poole, 2015; Rubino, 2015; Wouters et al., 2010). It is known that both $Hg(II)$ and $MeHg$ have a high affinity for reduced sulfur groups such as thiols (R-SH), monosulfides (R-S-R), and disulfides (R-SS-R) (Skylberg, 2010; Skylberg, 2012; Song et al., 2018; Taube et al., 2008). Moreover, both Hg species have a higher affinity for thiols than for disulfides (Liem-Nguyen, 2016; Yoon et al., 2005). We suggest that higher amounts of disulfides were present in the MCs amended with BC200 and BC500 whose disulfide bonds were reduced to the corresponding thiols leading to higher Hg_t sorption compared to CS. Following this assertion, Hg formed strong dissolved complexes with organic and inorganic ligands upon flooding while Hg was less attracted by potential binding sites of the biochars and the soil. Due to the strong attraction of the vicinal thiol pairs Hg could be removed from slurry when E_H changes induced the cleavage of existing disulfide bonds located on the surface of the biochars. This assertion is in good agreement with He et al. (2012) who indicated that a competitive complexation of Hg with DOC may limit the interactions of Hg with sorbents and who

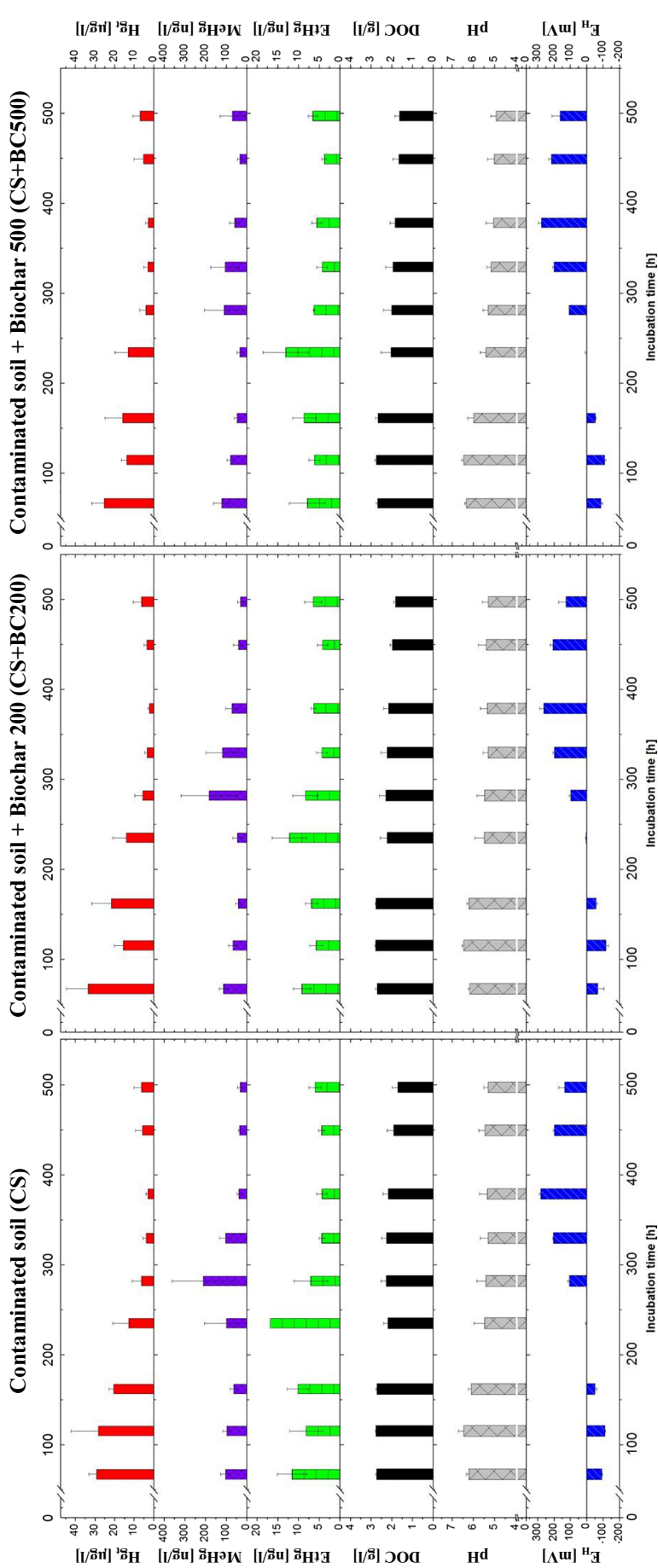


Fig. 2. Impact of pre-defined E_{Hr} -conditions on release dynamics of dissolved total Hg (Hg_t), methylmercury (MeHg), ethylmercury (EtHg), dissolved organic carbon (DOC), and pH in a contaminated soil (CS) compared with a contaminated soil treated with biochar pyrolyzed at 200 °C (CS + BC200) and a contaminated soil treated with biochar pyrolyzed at 500 °C (CS + BC500). Columns represent mean and whiskers represent standard deviation of four replicates using biogeochemical microcosm systems.

Table 3

Correlation coefficients (Pearson) between total dissolved mercury (Hg_t), mercury species (MeHg and EtHg) and factors controlling their release dynamics (E_H , pH 6, DOC, SUVA₂₅₄, Cl^- , SO_4^{2-} , Fe, Mn) ($n = 36$) of the contaminated soil (CS), the contaminated soil + Biochar 200 (CS + BC200), and the contaminated soil + Biochar 500 (CS + BC500).

Element	Soil	E_H 6	pH 6	DOC	SUVA ₂₅₄	Cl^-	SO_4^{2-}	Fe	Mn	EtHg	MeHg
Hg_t	CS	-0.804 ^a	0.845 ^a	0.710 ^a	0.559 ^a	-0.603 ^a	n.s.	n.s.	-0.763 ^a	0.737 ^{a,3}	n.s.
	CS + BC200	-0.685 ^a	0.664 ^a	0.638 ^a	0.344 ^b	-0.537 ^a	n.s.	n.s.	-0.618 ^a	0.530 ^{a,2}	n.s.
	CS + BC500	-0.728 ^{a,2}	0.759 ^{a,2}	0.734 ^{a,2}	n.s.	-0.453 ^{a,2}	n.s.	n.s.	-0.786 ^{a,2}	0.609 ^{a,4}	n.s.
MeHg	CS	n.s.	n.s.	0.357 ^{b,1}	n.s.	n.s.	n.s.	n.s.	n.s.	0.547 ^{a,3}	-
	CS + BC200	n.s.	n.s.	n.s.	n.s.	n.s.	n.s.	n.s.	n.s.	n.s.	-
	CS + BC500	n.s.	0.343 ^{b,2}	0.457 ^{a,2}	n.s.	n.s.	0.457 ^{a,2}	n.s.	-0.530 ^{a,2}	n.s.	-
EtHg	CS	-0.626 ^{a,3}	0.540 ^{a,3}	0.463 ^{a,3}	0.376 ^{b,3}	-0.530 ^{a,3}	n.s.	n.s.	-0.532 ^{a,3}	-	-
	CS + BC200	n.s.	n.s.	n.s.	n.s.	n.s.	n.s.	0.458 ^{b,2}	-0.364 ^{b,2}	-	-
	CS + BC500	-0.383 ^{b,4}	n.s.	0.367 ^{b,4}	n.s.	n.s.	n.s.	n.s.	-0.362 ^{b,4}	-	-

¹: $n = 35$; ²: $n = 34$; ³: $n = 33$; ⁴: $n = 32$.

n.s. = not significant.

DOC: dissolved organic carbon; SUVA₂₅₄: specific UV absorbance at 254 nm; SO_4^{2-} : sulfate.

^a Correlation significant at 0.01 level.

^b Correlation significant at 0.05 level.

attributed rapid adsorption of Hg to the binding of one Hg to two thiols. Moreover, while carboxyl (R-COOH) and hydroxyl groups (R-OH) are generally accepted as predominant biochar binding sites for heavy metals it has been shown that thiol-functionalized sorbents, including biochars, have a higher adsorption capacity and stronger selectivity for Hg (Huang et al., 2019; Niu et al., 2014; Xu et al., 2016). Adsorption kinetics and isotherms of such studies frequently suggest that thiol-functionalization improves the Hg species removal efficiency from aqueous solution considerably (e.g. Xia et al., 2019).

The observed concentrations of Hg_t released in CS (1.8–52 $\mu\text{g/l}$) greatly exceed levels reported for natural uncontaminated fresh water systems, and are comparable to higher concentrations reported in Hg mine drainage (Leopold et al., 2010; Rytuba, 2000). Thus, flooding and the alteration of E_H resulted in a substantial Hg_t release from CS which exceeds the U.S. Environmental Protection Agency's Maximum Contaminant Level for Hg in drinking water (2 $\mu\text{g/l}$) and the trigger value for the assessment of the soil – groundwater pathway (1 $\mu\text{g/l}$) of the German BBodSchV (1999).

3.2.2. Impact of E_H /pH changes on mobilization of MeHg in CS, CS + BC200, and CS + BC500

The pattern of MeHg concentrations was similar in CS and the biochar treatments (Fig. 2). In contrast to Hg_t no impact of biochar amendments was found under highly reduced conditions. This does not necessarily contradict the suggested cleavage of disulfide bonds as Skyllberg (2012) noted that there are indications that Hg and MeHg may bind to different types of thiol groups.

We did not find a correlation between MeHg and the E_H in CS, CS + BC200, or CS + BC500. Even though the methylation of Hg occurs primarily under anaerobic conditions, significant correlations between MeHg and E_H are not always observed (DeLaune et al., 2004; Frohne et al., 2012; Roulet et al., 2001; Sunderland et al., 2006). A positive correlation was detected between MeHg and pH in CS + BC500 (Table 3). An inverse relationship between these parameters is often reported (Ullrich et al., 2001). Golding et al. (2008) indicated that increased concentrations of Hg(II) within methylating bacteria due to declining pH values would probably be reflected in enhanced methylation activity. It is generally accepted that Hg methylation is primarily driven by microbial activity. Sulfate-reducing bacteria were identified as the principal methylators of Hg in sediments of various ecosystems primarily under anaerobic conditions (Beckers and Rinklebe, 2017; Boyd et al., 2017; Moreau et al., 2015). However, not all bacteria of the SRB phylogenetic tree methylate Hg (Barkay and Wagner-Döbler, 2005; Parks et al., 2013). It is suggested that SRB perform SO_4^{2-} reduction principally under highly reducing conditions at E_H s between -100 and -1000 mV (Dominique et al., 2007; Fritsche et al., 2014). Still, MeHg

concentrations determined in the course of the first three samplings under low E_H seem to be the result of soil-bound MeHg release rather than bacterial MeHg formation. Following the first sampling MeHg concentrations decreased in CS and the biochar treatments despite the lower E_H at the following sampling. Thus, MeHg that was bound to fine organic material may have initially entered the aqueous phase upon flooding, and was demethylated or sorbed over the course of the next two to three samplings. The release of sorbed MeHg when dry soils or sediments are flooded has been reported in previous studies (Bachand et al., 2014; Cesario et al., 2017; Marvin-DiPasquale et al., 2014). We found that net methylation started between the E_H windows of -50 mV and 0 mV and was highest between the E_H windows of 0 mV and 100 mV in CS and the biochar treatments (Fig. 2). This falls into the range of -100 to 100 mV identified by Windham-Myers et al. (2009) for high rates of MeHg production.

The ratio of SO_4^{2-} to Cl^- can be used as an indicator of SO_4^{2-} reduction (Alpers et al., 2014). Clear declines in this ratio were observed between E_H window -50 mV and 0 mV for CS and the biochar treatments, which corresponds well with the increase of MeHg concentrations. Furthermore, the ratio of MeHg to Hg_t increased 4.0 to 7.8 fold between E_H window 0 mV and 100 mV for the CS and biochar treatments, which represented the highest increase. This ratio is a frequently used indicator of methylation efficiency (Alpers et al., 2014; Frohne et al., 2012). High MeHg/ Hg_t rates indicate that available Hg is efficiently methylated while low MeHg/ Hg_t rates indicate either low Hg methylation or high demethylation rates (Remy et al., 2006). Thus, the increase in MeHg within CS and the biochar treatments fell within the range of Fe(III) reduction while the SO_4^{2-}/Cl^- ratio indicated that SO_4^{2-} reduction might have occurred (DeLaune and Reddy, 2005). It is well established that certain strains of iron-reducing bacteria (FeRB), such as *Geobacter* sp. strain CLFeRB, are also capable of methylating Hg, while methanogens that are known to demethylate MeHg may turn into the primary methylators under specific environmental conditions (Christensen et al., 2018; Fleming et al., 2006; Hamelin et al., 2011). Concentrations of dissolved Fe increased in the range of Fe(III) reduction around 0 mV (see Supporting Information) which may occur from microbial and chemical reduction of Fe(III) bearing minerals, such as Fe-oxides (Praharaaj and Fortin, 2008). The microbial reduction of Fe (III) bearing minerals is related to the activity of FeRB, which relies on the availability of labile organic C substrates and the abundance and crystallinity of Fe(III) bearing minerals (Praharaaj and Fortin, 2008; Roden, 2003). Abiotic Fe(III) reduction is indirectly controlled by the microbial SO_4^{2-} reduction, which is accompanied by the formation of sulfide species such as hydrogen sulfide that can act as significant reductants of Fe oxides (Li et al., 2006; Lindsay et al., 2015; Lohmayer et al., 2014). In fact, it has been frequently found that Fe(II) production

was rather driven by biogenic sulfide Fe(III) reduction than by the activity of FeRB (Hansel et al., 2015; Kwon et al., 2014; Praharaj and Fortin, 2008). Moreover, even though SRB are generally described as anoxic and neutrophilic bacteria they are present (but probably not metabolically active) under aerobic conditions and can tolerate low pH (Giloteaux et al., 2013; Koschorreck, 2008; Miao et al., 2012). Praharaj and Fortin (2008) determined low SO_4^{2-} reduction rates at E_H values between 300 and 450 mV, indicating that SRB activity is not restricted to highly reduced environments. Thus, even though the increase in dissolved MeHg concentrations in our experiment did not fall into the E_H range usually considered for Hg methylation by SRB, we may conclude that the methylation of Hg in CS and the biochar treatments between -50 and 100 mV was most probably mediated by SRB. Furthermore, the increases in soluble Fe at E_H 0 mV may be attributed to abiotic Fe(III) reduction linked to SO_4^{2-} reduction. Measured MeHg concentrations are the result of ongoing methylation and demethylation processes (Lambertsson and Nilsson, 2006; Lazaro et al., 2016) and therefore MeHg concentrations determined for the samplings following E_H window 100 mV at higher E_H in our experiment (Fig. 2) may in part be explained by the persistence of MeHg after major net methylation of Hg had been taken place earlier. In fact, MeHg concentrations in CS and the biochar treatments declined to approximately half between first 100 mV and first 200 mV E_H window. Most MeHg in many aquatic environments is generated in the sediments since MeHg production is basically the product of microbial activity and Hg(II) bioavailability (Hintelmann, 2010). On the other hand demethylation rates within sediments are high as well, which leads to a standing MeHg pool that constitutes no $> 1\%$ of the Hg_t (Hintelmann, 2010; Randall et al., 2013). However, demethylation activity is virtually absent in water leading to the persistence of MeHg in the overlying water column (Hintelmann, 2010). Here, comparatively high MeHg concentrations were depleted within two days in the course of controlled E_H changes.

A correlation between MeHg and Hg_t was missing in CS and the biochar treatments. This might be because the amount of bioavailable Hg in Hg_t may vary and since it is suggested that the production of MeHg is limited by microbial methylation potential rather than by Hg bioavailability (Bowman et al., 2015; Feng et al., 2014; Frohne et al., 2012).

3.2.3. Impact of E_H /pH changes on mobilization of EtHg in CS, CS + BC200, and CS + BC500

The pattern of EtHg in CS and the biochar treatments was very similar. The highest mean concentrations were determined for E_H window 0 mV (Fig. 2). Thereafter, there was a decline in EtHg with increasing E_H values and a slight increase when E_H was lowered again at the end of the experiment. Corresponding to this pattern, negative correlations between EtHg and E_H were determined for CS and CS + BC500 (Table 3). The concentrations of dissolved EtHg in the treatments amended with BC200 or BC500 were not significantly lower than those found in CS which indicates the moderate influence of the biochars on EtHg dissolution/formation (Table 2). Thus, the potential of BC200 and BC500 as immobilization agents for Hg_t , MeHg, and EtHg in our experiment was very limited. Considering our limited understanding of EtHg dissolution/formation, sufficient EtHg binding sites may be present in CS that would lessen the impact of the introduced biochar binding sites.

A positive correlation between EtHg and pH was only found in CS. This correlation is consistent with Pelcová et al. (2010) who observed significant EtHg adsorption to river sediments at pH 3–4. However, calculated relations between EtHg and other parameters seemed to be influenced by the strong positive correlations found between EtHg and Hg_t in CS and the biochar treatments (Table 3). It appears that EtHg was either released by the same processes as Hg_t or that a certain ratio of Hg_t was converted to EtHg. Such correlation between dissolved Hg_t and EtHg concentrations has been observed before (unpublished data). However, the inverse relation of these two parameters at E_H window

0 mV indicates that the conditions between the E_H windows of -50 mV and 0 mV may favor the formation of EtHg. Hintelmann (2010) noted that EtHg is not very persistent and readily decomposes in the environment, which would indicate that the EtHg determined in the course of our experiment would be rather a product of EtHg formation than of the release of legacy EtHg. The process of EtHg formation and its behavior in the natural environment is not well understood; for example, data on a microbial formation of EtHg are lacking (Beckers and Rinklebe, 2017; Hintelmann, 2010). Nevertheless, Cai et al. (1997) and Mao et al. (2010) suggested that EtHg may occur widely in the environment based on detected EtHg in soil samples. Ethylmercury has been detected in soils and sediments while its concentrations in other environmental samples such as atmospheric particulates, water, plant, and fish are frequently below the detection limits of (e.g. Chen et al., 2015; Song et al., 2013). Fortmann et al. (1978) showed that EtHg can form in tissues of common dwarf garden pea (*Pisum sativum*) after exposure to elemental Hg vapor and suggested that MeHg and EtHg might both be metabolites of a single Hg pathway in the peas. In fact, we found high EtHg concentrations at 0 mV preceding high MeHg concentrations at 100 mV.

3.3. Impact of DOC, Cl^- , SO_4^{2-} , Fe, and Mn changes on mobilization of Hg_t , MeHg, and EtHg in CS, CS + BC200, and CS + BC500

Similar to Hg_t the highest DOC concentrations were determined for those E_H windows sampled at the beginning of the experiment under low E_H conditions (Fig. 2). Therefore, we found positive correlations between Hg_t and DOC for CS and the biochar treatments (Table 3). Such correlations are frequently reported in literature (Bravo et al., 2018; Burns et al., 2013; Dittman et al., 2010) and DOC is generally regarded as the predominant ligand for both Hg_t and MeHg in oxic (sulfide-free) waters (Chadwick et al., 2013; Gorski et al., 2008; Ravichandran, 2004). However, positive relationships between Hg_t and DOC have been observed in numerous aquatic ecosystems and this link has been principally attributed to the strong affinity of Hg_t for reactive (reduced) thiol functional groups within DOC (Frohne et al., 2012; Ravichandran, 2004; Tsui and Finlay, 2011). Such a positive correlation may not always be detected, since the binding is controlled by a small fraction of dissolved organic matter molecules that contain these thiol groups (Ravichandran, 2004). In contrast, a positive correlation between Hg_t and DOC is generally found when Hg_t is mainly derived from wetlands and soils, where Hg_t is discharged and cotransported bound to the organic carbon (Wallschläger et al., 1996). This pattern is in good agreement with our results regarding Hg_t and DOC concentrations in CS and CS + BC200 and CS + BC500. Correlations in CS and the biochar treatments between either Hg_t or DOC with Fe or Mn were either missing or negative indicating that the release of Hg_t or DOC at low E_H was not governed by the reductive dissolution of particulate Fe and Mn oxyhydroxides and the release of associated Hg or DOC (Table 3). Instead, the results suggest that fine biologically decomposed organic material with associated Hg entered the aqueous phase upon flooding of the soil. Fig. 3 indicates a strong dependence of dissolved Hg_t on DOC and E_H with higher DOC concentrations and lower E_H values favoring Hg mobilization in CS, CS + BC200, and CS + BC500.

Total Hg concentrations in CS and the biochar treatments were also negatively correlated with Cl^- (Table 3). This relationship has been reported before (Hall et al., 2008).

Fig. 4 shows that lower Cl^- concentrations may have promoted the mobilization of Hg in CS, CS + BC200, and CS + BC500. Higher Cl^- concentrations may provoke the formation and precipitation of Hg_2Cl_2 thereby removing dissolved Hg (Chen et al., 2017; Kim et al., 2004).

Methylmercury was positively correlated with DOC in CS and in CS + BC500 (Table 3). As in the case with Hg_t it has been suggested that the aromaticity of DOC, calculated as SUVA_{254} values, may influence this relationship as higher aromaticity seems to enhance the Hg binding affinity or the number of strong binding sites (Tsui and Finlay,

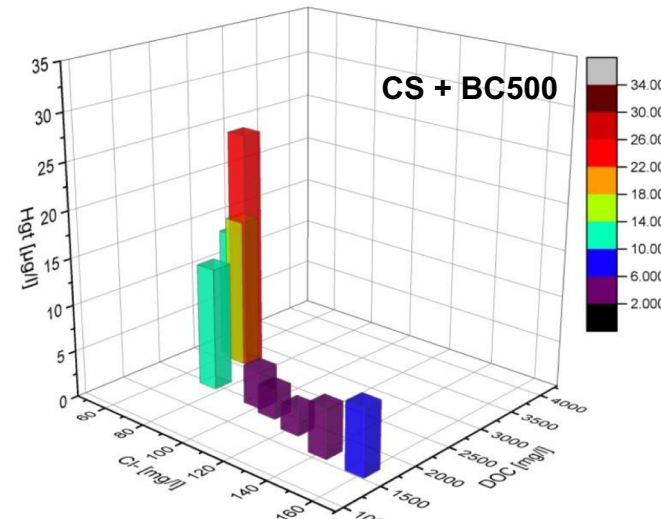
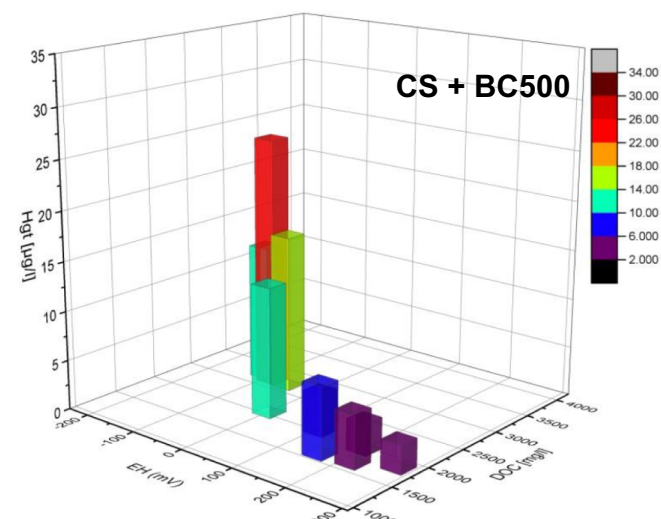
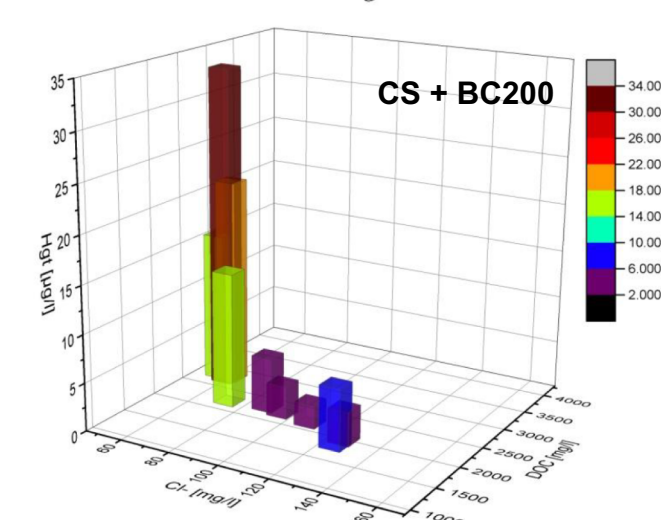
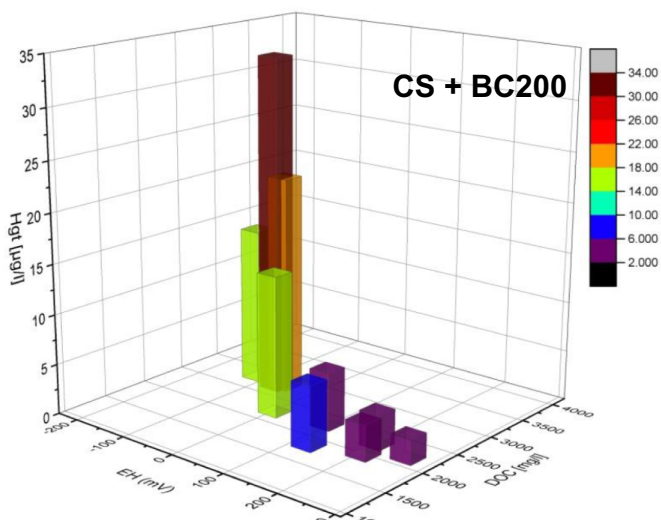
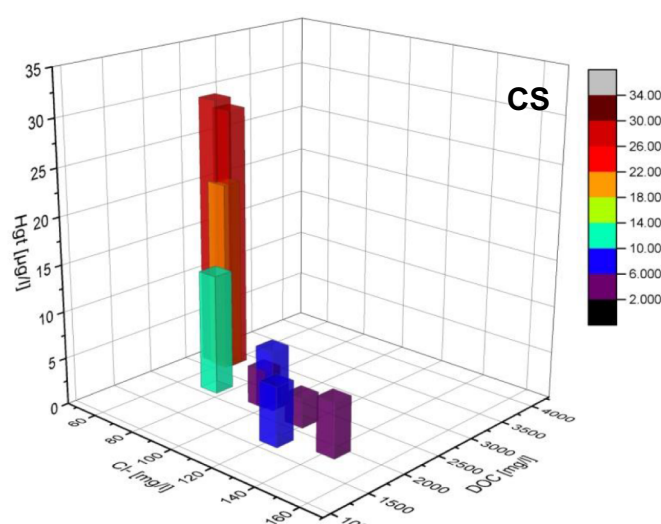
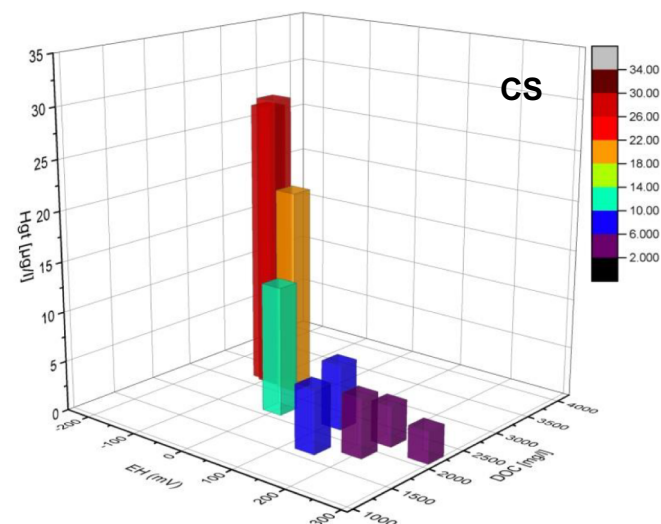


Fig. 3. Dependency of Hg_t concentrations in soil solution from redox potential (E_H) and DOC displayed in a three-dimensional coordinate system. Bars show means of data obtained for CS, CS + BC200, and CS + BC500. Bar colors correspond to the concentrations indicated by the color scale.

2011). It has been hypothesized that $SUVA_{254}$ may be a suitable predictor of dissolved Hg_t concentrations in certain streams (Burns et al., 2013). $SUVA_{254}$ has been found to be a useful indicator to assess the

Fig. 4. Dependency of Hg_t concentrations in soil solution from chloride concentrations (Cl^-) and DOC displayed in a three-dimensional coordinate system. Bars show means of data obtained for CS, CS + BC200, and CS + BC500. Bar colors correspond to the concentrations indicated by the color scale.

dissolved aromatic carbon content (Ravichandran et al., 1998; Weishaar et al., 2003). Some sources of interferences in the absorbance spectroscopy have to be considered (Li and Hur, 2017). Nitrate and

particularly ferric iron (Fe(III)) can exert a strong influence (Poulin et al., 2014; Weishaar et al., 2003). Under our experimental E_H -pH-conditions Fe should have been present as ferrous iron (Fe(II)) predominantly (Table 3) (Takeno, 2005) while nitrate concentrations were frequently below the detection limit.

Positive correlations between both Hg_t and MeHg with $SUVA_{254}$ have been reported for some aquatic ecosystems and biota (Chasar et al., 2009; Hall et al., 2008), but this strong relationship is not universal (Burns and Riva-Murray, 2018; Jiang et al., 2017b). The pattern of $SUVA_{254}$ values was similar between CS and the biochar treatments (Fig. S1). Correspondingly, strong correlations between $SUVA_{254}$ and Hg_t , MeHg, or EtHg were neither found in CS nor in the biochar treatments (Table 3). In general, $SUVA_{254}$ values were low compared to values reported for wetlands, rice fields, and lakes (Fleck et al., 2014; Poulin et al., 2014), water soluble organic matter (Jiang et al., 2017a), or porewater (Strickman and Mitchell, 2018).

Surprisingly, we found a positive correlation between MeHg and SO_4^{2-} in CS + BC500. Increasing concentrations of MeHg are usually concomitant with decreasing SO_4^{2-} concentrations (Hellal et al., 2015). Sulfate-reducing bacteria use SO_4^{2-} as a terminal electron acceptor for the degradation of organic compounds which leads to the depletion of SO_4^{2-} as well as the production and release of sulfide, which may result in the formation of MeHg as SRB species are capable of Hg methylation (Hellal et al., 2015; Lindsay et al., 2015; Muyzer and Stams, 2008). However, Liu et al. (2016) found that biochars may release SO_4^{2-} to solutions, with wood-based biochars releasing lower concentrations in CS + BC200 and CS + BC500 compared to CS and the correlation found between MeHg and SO_4^{2-} in CS + BC500 (Fig. S1, Tables 2, 3). The additional supply of SO_4^{2-} and labile organic carbon due to the amendment with biochar is considered to potentially promote Hg methylation (Liu et al., 2016). On the other hand, higher concentrations of SO_4^{2-} may inhibit MeHg production due to the formation of H_2S (Shao et al., 2012). Microbial SO_4^{2-} reduction can be inhibited by H_2S and organic acids which can be toxic for the SRB even though H_2S is produced by the SRB in the course of their energy metabolism (Koschorreck, 2008). In addition, methylation rates were found to be lower under high sulfide concentrations and the presence of FeS due to a shift from neutral Hg(II)-sulfide complexes, which are easily taken up by bacteria, to charged Hg(II)-polysulfide (Hellal et al., 2015; Liu et al., 2008). We may therefore conclude that the little additional SO_4^{2-} that was likely released due to the biochar amendments had no relevant effect on MeHg production.

Correlations between EtHg and SO_4^{2-} were missing in CS and the biochar treatments (Table 3). It has been indicated that SO_4^{2-} may affect the adsorption of EtHg: Chen et al. (2015) observed that the adsorption of EtHg to sediments decreased in line with SO_4^{2-} addition. However, Pelcová et al. (2010) increased the SO_4^{2-} concentration in solution to 50 and 200 mg/l, respectively and found only slight differences in EtHg adsorption between these two concentrations.

3.4. Factor analyses

Factor analyses were performed for CS and the biochar treatments (Fig. 5) to evaluate associations between the measured parameters and to identify hidden multivariate data structures. We extracted two factors. These factors explained 65.45% of the total variance in CS (48.86% Component No. 1 and 16.59% Component No. 2), 61.33% in CS + BC200 (46.49% Component No. 1 and 14.84% Component No. 2), and 64.32% in CS + BC500 (48.50% Component No. 1 and 15.82% Component No. 2), respectively.

Fig. 5A shows that Hg_t , EtHg, DOC, and pH had high loadings on Component No. 1 in CS which indicates a similar biogeochemical behavior of these parameters. Manganese and E_H , in contrast, had high negative loadings on Component No. 1 which demonstrates their opposing behavior. Sulfate and $SUVA_{254}$ clustered together and had high

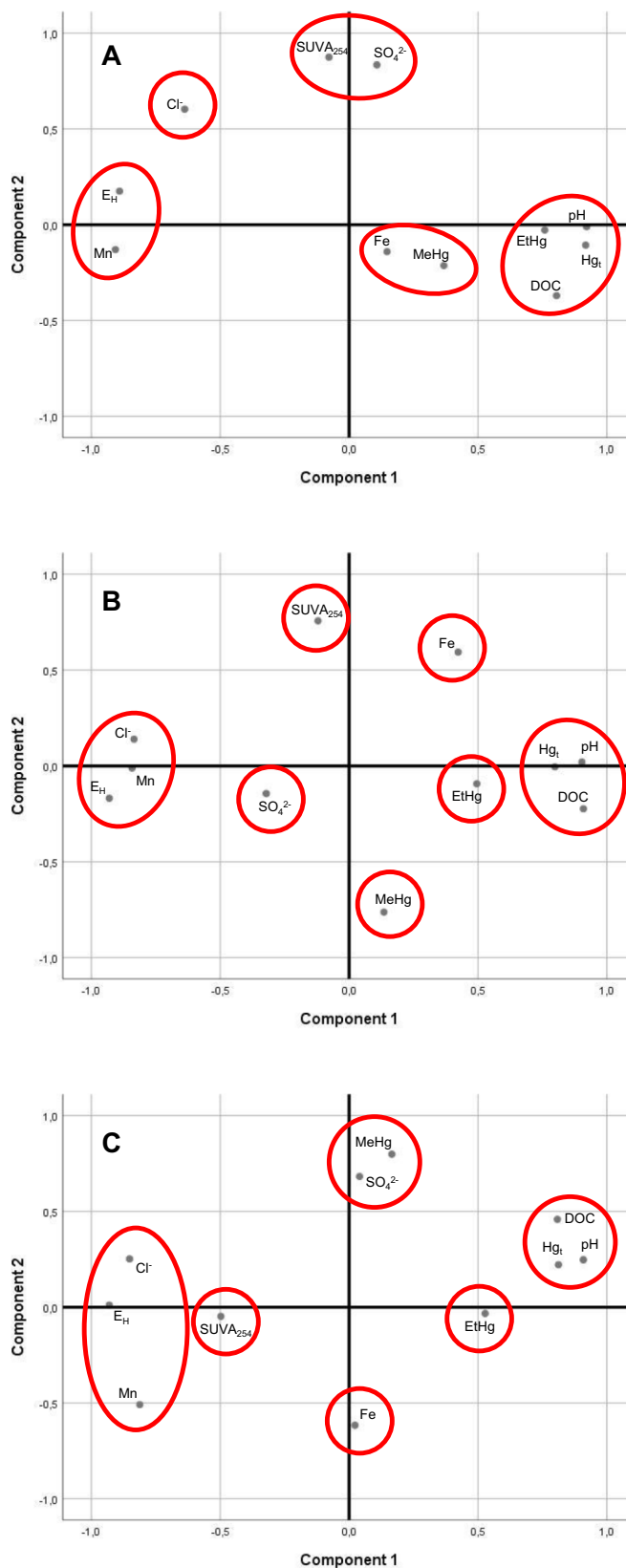
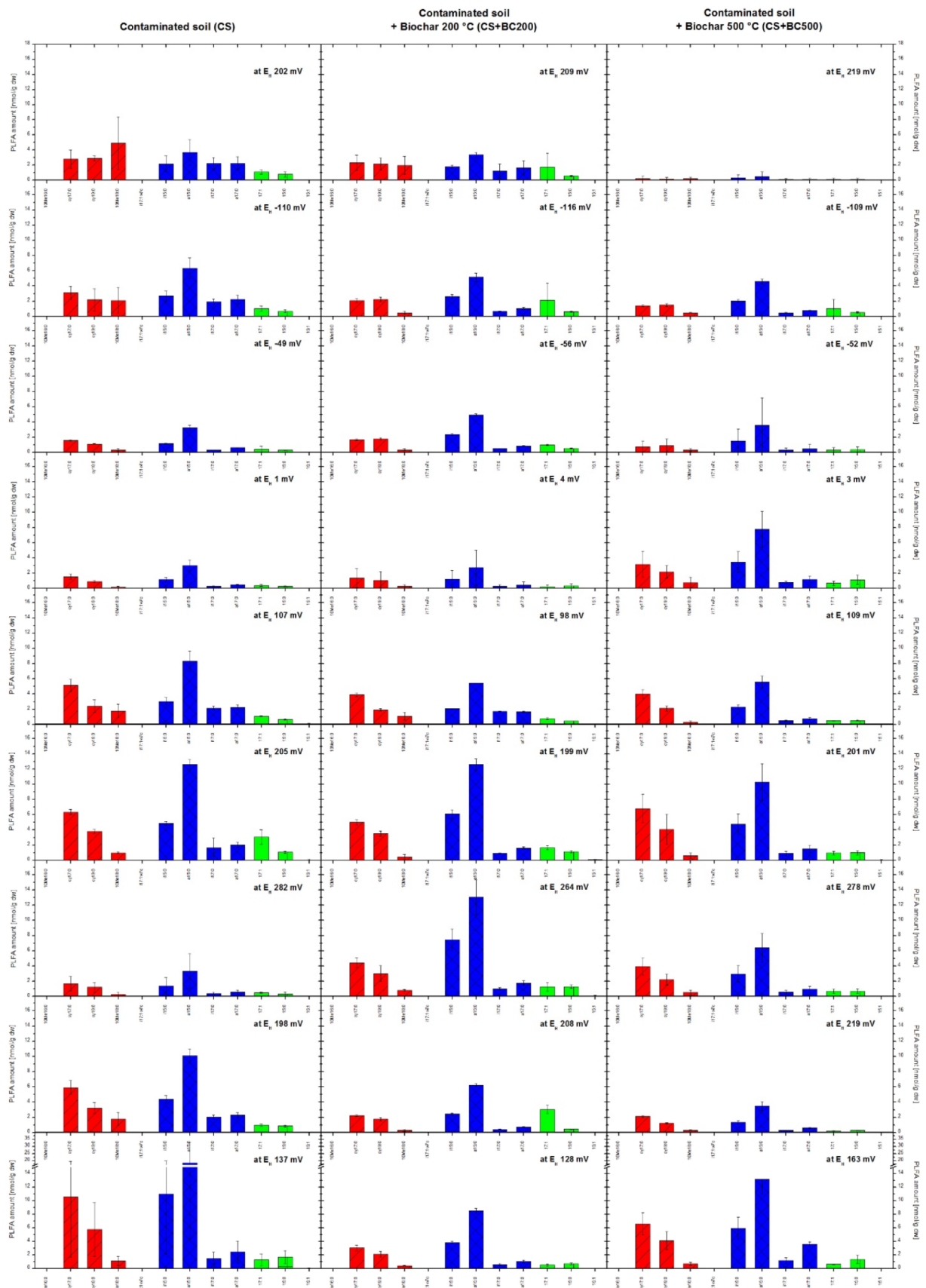


Fig. 5. Factor analysis of the contaminated soil (CS), the contaminated soil + biochar pyrolyzed at 200 °C (CS + BC200), and contaminated soil + biochar pyrolyzed at 500 °C (CS + BC500). Kaiser-Meyer-Olkin (KMO) measures were 0.636 for CS, 0.585 for CS + BC200, and 0.699 for CS + BC500, respectively.



A B C D E F G H J K L M A B C D E F G H J K L M A B C D E F G H J K L M
 A, 10Me16:0; B, cy17:0; C, cy19:0; D, 10Me18:0; E, i17:1ω7c; F, i15:0; G, a15:0; H, i17:0; J, a17:0;
 K, 17:1; L, 15:0; M, 15:1

Fig. 6. SRB PLFA amounts as influenced by soil treatment and changing E_H /pH.

loadings on Component No. 2. Chloride, MeHg and Fe showed less intense loading on the two components, suggesting that they were presumably best explained by other components. In CS + BC200 (Fig. 5B) and CS + BC500 (Fig. 5C) Hg_t, DOC, and pH were again clustered together. Furthermore, Mn and E_H, which clustered with Cl⁻, indicated again dissimilar biogeochemical behavior. Other parameters such as EtHg, Fe, and SUVA₂₅₄ were ungrouped. Summarizing, the results of the factor analyses indicate similarities in the biogeochemical behavior of Hg_t and DOC, while Mn was linked to E_H regardless of whether CS was amended or not. Neither amendment, BC200 or BC500, resulted in pronounced effects on the interrelationships of the parameters.

3.5. Impact of E_H/pH changes on the microbial community

Fifty-five PLFAs were detected. Forty-five of them had carbon numbers between C₁₂ and C₂₀. Bacteria contain fatty acids mainly in this chain length range (Frostegård and Bååth, 1996; Jiang et al., 2012; White et al., 1996) (Fig. S2, see Supporting information). In general, changes in abundances of PLFAs considered for the SRB and those with carbon numbers between C₁₂ and C₂₀ were similar (Figs. 6, S2).

Phospholipid fatty acid abundances in the initial samples taken subsequent to the flooding of the soils when E_H was around 210 mV were slightly higher in CS compared to CS + BC200, while the amount of PLFAs detected in CS + BC500 was considerably lower (Fig. 6). Thus, the added BC500 seems to have had an important impact on the soil microbial community at this stage of the experiment, presumably due to its smooth surface and the shortage of nutrients which may have impeded its microbial colonization. The *Desulfobacter* biomarker fatty acid 10Me16:0 was absent in CS and the biochar treated soils over the course of the experiment (Fig. 6). However, the suitability of 10Me16:0 as a *Desulfobacter* specific biomarker has been questioned (Parkes et al., 1993). Similarly, *Desulfovibrio* biomarker i17:1ω7c was not detected, while the considered *Desulfovibrio* indicator fatty acid 17:1ω6 could not be determined individually but as part of the summed aggregate 17:1. The abundances of PLFAs considered for the SRB were comparable between CS and the biochar treatments at the lowest sampled E_H around -110 mV. Clear changes in PLFA abundance were found for 10Me18:0 (decrease) and a15:0 (increase). Increasing E_H to 0 mV resulted in decreasing PLFA abundances in CS and CS + BC200, while this effect was not observed in CS + BC500 (Fig. 6). The results for the E_H windows 100 mV and 200 mV were very similar in CS and the biochar treatments. In general, PLFA abundances increased. Distinct decreases in PLFA abundance were found for CS and CS + BC500 at E_H window 300 mV. Lowering the E_H to 200 mV again resulted in PLFA abundances that were comparable to the first sampled 200 mV window in CS. However, PLFA abundances had decreased considerably in CS + BC200 and CS + BC500 at the same time (Fig. 6). Abundances for the last sampling were again higher in CS and the biochar treatments.

In general, PLFA results gave no clear indication of whether SRB were the likely Hg methylators in our experiment. However, the concomitant increase in “SRB” PLFA abundance and MeHg concentrations at the first 100 mV E_H window may be seen as a sign of SRB mediated Hg methylation (Figs. 2, 6).

4. Conclusions

We aimed to study the impact of two different biochars as amendments to a contaminated floodplain soil on the release of Hg_t as well as the formation and mobilization of MeHg and EtHg under dynamic E_H conditions utilizing an advanced automated biogeochemical microcosm system. Both amendments, BC200 and BC500, showed little impact on the mobilization of Hg_t, MeHg, and EtHg as well as on redox processes. Although BC500 was somewhat more effective than BC200 in controlling the mobilization of Hg_t and MeHg the results were marginal. This may reflect the formation of strong Hg complexes with dissolved organic and inorganic ligands under our experimental conditions, leading

to a minor formation of chemical bonds between Hg and functional groups of the biochars. Therefore, the high Hg_t, MeHg, and EtHg concentrations at the beginning of the experiment at E_H windows ~ -80 mV and -110 mV might be interpreted as co-dissolution of Hg and DOC upon flooding, rather than a direct effect of lowering E_H at the beginning of the experiment. This assertion is supported by the strong correlations between Hg_t, MeHg, and EtHg with DOC and declining Hg concentrations despite declining E_H. Secondly, biochar is known to possess a large number of negative surface charges, which should actually be able to sorb Hg²⁺. However, it could be that those potential binding sites for Hg at the biochar itself may have been occupied by other ions and/or blocked by biofilm that may have led to a mobilization of Hg and its compounds. Therefore, Hg_t could be mobilized in CS + BC200 and CS + BC500 to a similar extent as compared to CS. Overall, the mobilization of Hg_t, MeHg, and EtHg was largely impacted by the systematic changes in E_H. We found an inverse relationship between E_H and Hg_t while the impact of E_H on MeHg and EtHg concentrations was rather characterized by specific E_H windows at which ethylation (0 mV) and methylation (between -50 and 100 mV) were favored. Presumably SRB were the principal methylators in our experiment based on PLFA results.

Future research should further clarify the impact of E_H and DOC on Hg mobilization and the role of Cl⁻ in influencing Hg_t immobilization. Thorough microbial analyses should be conducted to better evaluate the role of SRB. Additionally, the complex interactions between biochar and soil biogeochemical redox processes should be further elucidated. Also, various biochars, differing in feedstock and pyrolysis temperature as well as designed biochars should be tested with a view to their potential to decrease the mobilization of Hg_t, MeHg, and EtHg under dynamic redox conditions in frequently flooded soils. Finally, considering the high Hg_t release, our study highlights the necessity of conducting amendment tests under variable redox conditions in the field to evaluate the severity of environmental risk.

Supplementary data to this article can be found online at <https://doi.org/10.1016/j.envint.2019.03.040>.

Acknowledgments

The authors thank Mrs. Sandra Scharfenort and Mr. Claus Vandenhirtz (University of Wuppertal, Germany) for technical assistance as well as Mrs. Julia Staiger for measuring the PLFA. Furthermore, we would like to thank three anonymous reviewers as well as Prof. John Seaman for their thoughtful comments and suggestions, which helped to improve the quality of this paper.

References

- Ahmad, M., Rajapaksha, A.U., Lim, J.E., Zhang, M., Bolan, N., Mohan, D., Vithanage, M., Lee, S.S., Ok, Y.S., 2014. Biochar as a sorbent for contaminant management in soil and water: a review. *Chemosphere* 99, 19–33.
- Ahmad, M., Lee, S.S., Lee, S.E., Al-Wabel, M.I., Tsang, D.C.W., Ok, Y.S., 2017. Biochar-induced changes in soil properties affected immobilization/mobilization of metals/metalloids in contaminated soils. *J. Soils Sediments* 17, 717–730.
- Alpers, C.N., Fleck, J.A., Marvin-DiPasquale, M., Stricker, C.A., Stephenson, M., Taylor, H.E., 2014. Mercury cycling in agricultural and managed wetlands, Yolo Bypass, California: spatial and seasonal variations in water quality. *Sci. Total Environ.* 484, 276–287.
- Bachand, P.A.M., Bachand, S.M., Fleck, J.A., Alpers, C.N., Stephenson, M., Windham-Myers, L., 2014. Reprint of “methylmercury production in and export from agricultural wetlands in California, USA: the need to account for physical transport processes into and out of the root zone”. *Sci. Total Environ.* 484, 249–262.
- Bakir, F., Damluji, S.F., Amin-Zaki, L., Murtadha, M., Khalidi, A., Al-Rawi, N.Y., Tikriti, S., Dhahir, H.I., Clarkson, T.W., Smith, J.C., Doherty, R.A., 1973. Methylmercury Poisoning in Iraq. *Science* 181, 230–241.
- Barkay, T., Wagner-Döbler, I., 2005. Microbial Transformations of Mercury: Potentials, Challenges, and Achievements in Controlling Mercury Toxicity in the Environment. *Advances in Applied Microbiology*. Academic Press.
- Barrow, N.J., Cox, V.C., 1992. The effects of pH and chloride concentration on mercury sorption. II. By a soil. *J. Soil Sci.* 43, 305–312.
- BBodSchV, 1999. In: Federal Government (Ed.), Federal Soil Protection and Contaminated Sites Ordinance (BBodSchV). Federal Government, Bonn.

- Beckers, F., Rinklebe, J., 2017. Cycling of mercury in the environment: sources, fate, and human health implications: a review. *Crit. Rev. Environ. Sci. Technol.* 47, 693–794.
- Beesley, L., Moreno-Jimenez, E., Gomez-Eyles, J.L., 2010. Effects of biochar and green-waste compost amendments on mobility, bioavailability and toxicity of inorganic and organic contaminants in a multi-element polluted soil. *Environ. Pollut.* 158, 2282–2287.
- Beiyuan, J., Awad, Y.M., Beckers, F., Tsang, D.C., Ok, Y.S., Rinklebe, J., 2017. Mobility and phytoavailability of As and Pb in a contaminated soil using pine sawdust biochar under systematic change of redox conditions. *Chemosphere* 178, 110–118.
- Blume, H.-P., Stahr, K., Leinweber, P., 2011. *Bodenkundliches Praktikum. Eine Einführung in pedologisches Arbeiten für Ökologen, Land- und Forstwirte, Geo- und Umweltwissenschaftler*. 3. Springer Spektrum, Heidelberg.
- Bohn, H.L., 1971. Redox potentials. *Soil Sci.* 112, 39–45.
- Bowman, K.L., Hammerschmidt, C.R., Lamborg, C.H., Swarr, G., 2015. Mercury in the North Atlantic Ocean: the U.S. GEOTRACES zonal and meridional sections. *Deep-Sea Res. II Top. Stud. Oceanogr.* 116, 251–261.
- Boyd, E.S., Yu, R.Q., Barkay, T., Hamilton, T.L., Baxter, B.K., Naftz, D.L., Marvin-DiPasquale, M., 2017. Effect of salinity on mercury methylating benthic microbes and their activities in Great Salt Lake, Utah. *Sci. Total Environ.* 581–582, 495–506.
- Bravo, A.G., Kothawala, D.N., Attermeyer, K., Tessier, E., Bodmer, P., Ledesma, J.L.J., Audet, J., Casas-Ruiz, J.P., Catalan, N., Cuvy-Fraunie, S., Colls, M., Deininger, A., Evtimova, V.V., Fonvielle, J.A., Fuss, T., Gilbert, P., Herrero Ortega, S., Liu, L., Mendoza-Lera, C., Monteiro, J., Mor, J.R., Nagler, M., Niedrist, G.H., Nydahl, A.C., Pastor, A., Pegg, J., Gutmann Roberts, C., Pilotto, F., Portela, A.P., Gonzalez-Quijano, C.R., Romero, F., Rulik, M., Amouroux, D., 2018. The interplay between total mercury, methylmercury and dissolved organic matter in fluvial systems: a latitudinal study across Europe. *Water Res.* 144, 172–182.
- Burns, D.A., Riva-Murray, K., 2018. Variation in fish mercury concentrations in streams of the Adirondack region, New York: a simplified screening approach using chemical metrics. *Ecol. Indic.* 84, 648–661.
- Burns, D.A., Aiken, G.R., Bradley, P.M., Journey, C.A., Schelker, J., 2013. Specific ultraviolet absorbance as an indicator of mercury sources in an Adirondack River basin. *Biogeochemistry* 113, 451–466.
- Cai, Y., Jaffé, R., Jones, R., 1997. Ethylmercury in the soils and sediments of the Florida Everglades. *Environ. Sci. Technol.* 31, 302–305.
- Cassina, L., Tassi, E., Pedron, F., Petruzzelli, G., Ambrosini, P., Barbaferri, M., 2012. Using a plant hormone and a thioligand to improve phytoremediation of Hg-contaminated soil from a petrochemical plant. *J. Hazard. Mater.* 231–232, 36–42.
- Cesario, R., Poissant, L., Pilote, M., O'Driscoll, N.J., Mota, A.M., Canario, J., 2017. Dissolved gaseous mercury formation and mercury volatilization in intertidal sediments. *Sci. Total Environ.* 603–604, 279–289.
- Chadwick, S.P., Babiarez, C.L., Hurley, J.P., Armstrong, D.E., 2013. Importance of hypolimnetic cycling in aging of “new” mercury in a northern temperate lake. *Sci. Total Environ.* 448, 176–188.
- Chasar, L.C., Scudder, B.C., Stewart, A.R., Bell, A.H., Aiken, G.R., 2009. Mercury cycling in stream ecosystems. 3. Trophic dynamics and methylmercury bioaccumulation. *Environ. Sci. Technol.* 43, 2733–2739.
- Chen, B., Wu, Y., Guo, X., He, M., Hu, B., 2015. Speciation of mercury in various samples from the micro-ecosystem of East Lake by hollow fiber-liquid-liquid-liquid micro-extraction-HPLC-ICP-MS. *J. Anal. At. Spectrom.* 30, 875–881.
- Chen, Y., Yin, Y., Shi, J., Liu, G., Hu, L., Liu, J., Cai, Y., Jiang, G., 2017. Analytical methods, formation, and dissolution of cinnabar and its impact on environmental cycle of mercury. *Crit. Rev. Environ. Sci. Technol.* 47, 2415–2447.
- Chen, J., Wang, C., Pan, Y., Farzana, S.S., Tam, N.F., 2018. Biochar accelerates microbial reductive debromination of 2,2',4,4'-tetrabromodiphenyl ether (BDE-47) in anaerobic mangrove sediments. *J. Hazard. Mater.* 341, 177–186.
- Christensen, G.A., Somenahally, A.C., Moberly, J.G., Miller, C.M., King, A.J., Gilmour, C.C., Brown, S.D., Podar, M., Brandt, C.C., Brooks, S.C., Palumbo, A.V., Wall, J.D., Elias, D.A., 2018. Carbon amendments alter microbial community structure and net mercury methylation potential in sediments. *Appl. Environ. Microbiol.* 84.
- DeLaune, R.D.; Reddy, K.R. Redox potential in: Hillel D., ed. *Encyclopedia of Soils in the Environment*. Oxford: Elsevier; 2005.
- DeLaune, R.D., Jugsujinda, A., Devai, I., Patrick, W.H., 2004. Relationship of sediment redox conditions to methyl mercury in surface sediment of Louisiana Lakes. *J. Environ. Sci. Health A* 39, 1925–1933.
- Devai, I., Patrick, W.H., Neue, H.U., DeLaune, R.D., Kongchum, M., Rinklebe, J., 2005. Methyl mercury and heavy metal content in soils of Rivers Saale and Elbe (Germany). *Anal. Lett.* 38, 1037–1048.
- DIN EN 15933, 2012. Schlamm, behandelter Bioabfall und Boden – Bestimmung des pH-Werts. Deutsches Institut für Normung e. V., Berlin.
- Dittman, J.A., Shanley, J.B., Driscoll, C.T., Aiken, G.R., Chalmers, A.T., Towse, J.E., Selvendiran, P., 2010. Mercury dynamics in relation to dissolved organic carbon concentration and quality during high flow events in three northeastern U.S. streams. *Water Resour. Res.* 46 (n/a-n/a).
- Dominique, Y., Muresan, B., Duran, R., Richard, S., Boudou, A., 2007. Simulation of the chemical fate and bioavailability of liquid elemental mercury drops from gold mining in Amazonian Freshwater Systems. *Environ. Sci. Technol.* 41, 7322–7329.
- Dong, X., Ma, L.Q., Zhu, Y., Li, Y., Gu, B., 2013. Mechanistic investigation of mercury sorption by Brazilian pepper biochars of different pyrolytic temperatures based on X-ray photoelectron spectroscopy and flow calorimetry. *Environ. Sci. Technol.* 47, 12156–12164.
- Dranguet, P., Le Faucheur, S., Slaveykova, V.I., 2017. Mercury bioavailability, transformations, and effects on freshwater biofilms. *Environ. Toxicol. Chem.* 36, 3194–3205.
- Dranguet, P., Slaveykova, V.I., Le Faucheur, S., 2018. Kinetics of mercury accumulation by freshwater biofilms. *Environ. Chem.* 14, 458–467.
- Feng, Y., Motta, A.C., Reeves, D.W., Burmester, C.H., van Santen, E., Osborne, J.A., 2003. Soil microbial communities under conventional-till and no-till continuous cotton systems. *Soil Biol. Biochem.* 35, 1693–1703.
- Feng, S., Ai, Z., Zheng, S., Gu, B., Li, Y., 2014. Effects of dryout and inflow water quality on mercury methylation in a constructed wetland. *Water Air Soil Pollut.* 225.
- Fleck, J.A., Gill, G., Bergamaschi, B.A., Kraus, T.E., Downing, B.D., Alpers, C.N., 2014. Concurrent photolytic degradation of aqueous methylmercury and dissolved organic matter. *Sci. Total Environ.* 484, 263–275.
- Fleming, E.J., Mack, E.E., Green, P.G., Nelson, D.C., 2006. Mercury methylation from unexpected sources: molybdate-inhibited freshwater sediments and an iron-reducing bacterium. *Appl. Environ. Microbiol.* 72, 457–464.
- Fortmann, L., Gay, D., Wirtz, K., 1978. Ethylmercury: Formation in Plant Tissues and Relation to Methylmercury Formation. EPA, Washington, D.C.
- Fritsche, J., Osterwalder, S., Nilsson, M.B., Sagerfors, J., Åkerblom, S., Bishop, K., Alewell, C., 2014. Evasion of elemental mercury from a boreal peatland suppressed by long-term sulfate addition. *Environ. Sci. Technol. Lett.* 1, 421–425.
- Frohne, T., Rinklebe, J., 2013. Biogeochemical fractions of mercury in soil profiles of two different floodplain ecosystems in Germany. *Water Air Soil Pollut.* 224.
- Frohne, T., Rinklebe, J., Langer, U., Du Laing, G., Mothes, S., Wennrich, R., 2012. Biogeochemical factors affecting mercury methylation rate in two contaminated floodplain soils. *Biogeochemistry* 9, 493–507.
- Frostegård, A., Bååth, E., 1996. The use of phospholipid fatty acid analysis to estimate bacterial and fungal biomass in soil. *Biol. Fertil. Soils* 22, 59–65.
- Frostegård, Å., Tunlid, A., Bååth, E., 1991. Microbial biomass measured as total lipid phosphate in soils of different organic content. *J. Microbiol. Methods* 14, 151–163.
- Giloteaux, L., Duran, R., Casiot, C., Bruneel, O., Elbaz-Poulichet, F., Goni-Urriza, M., 2013. Three-year survey of sulfate-reducing bacteria community structure in Carnoules acid mine drainage (France), highly contaminated by arsenic. *FEMS Microbiol. Ecol.* 83, 724–737.
- Golding, G.R., Sparling, R., Kelly, C.A., 2008. Effect of pH on intracellular accumulation of trace concentrations of Hg(II) in *Escherichia coli* under anaerobic conditions, as measured using a mer-lux bioreporter. *Appl. Environ. Microbiol.* 74, 667–675.
- Gorski, P.R., Armstrong, D.E., Hurley, J.P., Krabbenhoft, D.P., 2008. Influence of natural dissolved organic carbon on the bioavailability of mercury to a freshwater alga. *Environ. Pollut.* 154, 116–123.
- Gross, R., Hauer, B., Otto, K., Schmid, A., 2007. Microbial biofilms: new catalysts for maximizing productivity of long-term biotransformations. *Biotechnol. Bioeng.* 98, 1123–1134.
- Haitzer, M., Aiken, G.R., Ryan, J.N., 2002. Binding of mercury(II) to dissolved organic matter: the role of the mercury-to-DOM concentration ratio. *Environ. Sci. Technol.* 36, 3564–3570.
- Hall, B.D., Aiken, G.R., Krabbenhoft, D.P., Marvin-DiPasquale, M., Swarzenski, C.M., 2008. Wetlands as principal zones of methylmercury production in southern Louisiana and the Gulf of Mexico region. *Environ. Pollut.* 154, 124–134.
- Hamelin, S., Amyot, M., Barkay, T., Wang, Y., Planas, D., 2011. Methanogens: principal methylators of mercury in lake periphyton. *Environ. Sci. Technol.* 45, 7693–7700.
- Han, F., 2007. *Biogeochemistry of Trace Elements in Arid Environments*. Springer, Dordrecht.
- Hansel, C.M., Lentini, C.J., Tang, Y., Johnston, D.T., Wankel, S.D., Jardine, P.M., 2015. Dominance of sulfur-fueled iron oxide reduction in low-sulfate freshwater sediments. *The ISME Journal* 9, 2400–2412.
- He, F., Wang, W., Moon, J.-W., Howe, J., Pierce, E.M., Liang, L., 2012. Rapid removal of Hg(II) from aqueous solutions using thiol-functionalized Zn-doped biomagnetite particles. *ACS Appl. Mater. Interfaces* 4, 4373–4379.
- Hellal, J., Guedron, S., Huguet, L., Schafer, J., Laperche, V., Joulain, C., Lancelour, L., Burnol, A., Ghestem, J.P., Garrido, F., Battaglia-Brunet, F., 2015. Mercury mobilization and speciation linked to bacterial iron oxide and sulfate reduction: a column study to mimic reactive transfer in an anoxic aquifer. *J. Contam. Hydrol.* 180, 56–68.
- Hintelmann, H., 2010. 11 Organomercurials. Their formation and pathways in the environment. In: *Organometallics in Environment and Toxicology: Metal Ions in Life Sciences*. The Royal Society of Chemistry.
- Hintelmann, H., Ebinghaus, R., Wilken, R.-D., 1993. Accumulation of mercury(II) and methylmercury by microbial biofilms. *Water Res.* 27, 237–242.
- Huang, Y., Xia, S., Lyu, J., Tang, J., 2019. Highly efficient removal of aqueous Hg²⁺ and CH₃Hg⁺ by selective modification of biochar with 3-mercaptopropyltrimethylxysilane. *Chem. Eng. J.* 360, 1646–1655.
- Hunter, D., Bomford, R.R., Russell, D.S., 1940. Poisoning by methyl mercury compounds. *QJM: An International Journal of Medicine* 9, 193–226.
- Igalavithana, A.D., Lee, S.E., Lee, Y.H., Tsang, D.C., Rinklebe, J., Kwon, E.E., Ok, Y.S., 2017. Heavy metal immobilization and microbial community abundance by vegetable waste and pine cone biochar of agricultural soils. *Chemosphere* 174, 593–603.
- IUSS, 2015. World Reference Base for Soil Resources 2014, Update 2015. International Soil Classification System for Naming Soils and Creating Legends for Soil Maps. FAO, Rome.
- Janssen, S.E., Schaefer, J.K., Barkay, T., Reinfelder, J.R., 2016. Fractionation of mercury stable isotopes during microbial methylmercury production by iron- and sulfate-reducing bacteria. *Environ. Sci. Technol.* 50, 8077–8083.
- Jiang, L., Cai, C., Zhang, Y., Mao, S., Sun, Y., Li, K., Xiang, L., Zhang, C., 2012. Lipids of sulfate-reducing bacteria and sulfur-oxidizing bacteria found in the Dongsheng uranium deposit. *Chin. Sci. Bull.* 57, 1311–1319.
- Jiang, T., Kaal, J., Liang, J., Zhang, Y., Wei, S., Wang, D., Green, N.W., 2017a. Composition of dissolved organic matter (DOM) from periodically submerged soils in the Three Gorges Reservoir areas as determined by elemental and optical analysis, infrared spectroscopy, pyrolysis-GC-MS and thermally assisted hydrolysis and methylation. *Sci. Total Environ.* 603–604, 461–471.
- Jiang, T., Skjylberg, U., Bjorn, E., Green, N.W., Tang, J., Wang, D., Gao, J., Li, C., 2017b. Characteristics of dissolved organic matter (DOM) and relationship with dissolved

- mercury in Xiaoqing River-Laizhou Bay estuary, Bohai Sea, China. *Environ. Pollut.* 223, 19–30.
- Jones, D.L., Rousk, J., Edwards-Jones, G., DeLuca, T.H., Murphy, D.V., 2012. Biochar-mediated changes in soil quality and plant growth in a three year field trial. *Soil Biol. Biochem.* 45, 113–124.
- Kammann, C.I., Schmidt, H.P., Messerschmidt, N., Linsel, S., Steffens, D., Muller, C., Koyro, H.W., Conte, P., Joseph, S., 2015. Plant growth improvement mediated by nitrate capture in co-composted biochar. *Sci. Rep.* 5, 11080.
- Kim, C.S., Rytuba, J.J., Brown, G.E., 2004. EXAFS study of mercury(II) sorption to Fe- and Al-(hydr)oxides. *J. Colloid Interface Sci.* 270, 9–20.
- Klasson, K.T., Boihem, L.L., Uchimiya, M., Lima, I.M., 2014. Influence of biochar pyrolysis temperature and post-treatment on the uptake of mercury from flue gas. *Fuel Process. Technol.* 123, 27–33.
- Klüpfel, L., Keiluweit, M., Kleber, M., Sander, M., 2014. Redox properties of plant biomass-derived black carbon (biochar). *Environ. Sci. Technol.* 48, 5601–5611.
- Kodamatani, H., Tomiyasu, T., 2013. Selective determination method for measurement of methylmercury and ethylmercury in soil/sediment samples using high-performance liquid chromatography-chemiluminescence detection coupled with simple extraction technique. *J. Chromatogr. A* 1288, 155–159.
- Kong, H., He, J., Gao, Y., Wu, H., Zhu, X., 2011. Cosorption of phenanthrene and mercury (II) from aqueous solution by soybean stalk-based biochar. *J. Agric. Food Chem.* 59, 12116–12123.
- Koschorreck, M., 2008. Microbial sulphate reduction at a low pH. *FEMS Microbiol. Ecol.* 64, 329–342.
- Kwon, M.J., Boyanov, M.I., Antonopoulos, D.A., Brulc, J.M., Johnston, E.R., Skinner, K.A., Kemner, K.M., O'Loughlin, E.J., 2014. Effects of dissimilatory sulfate reduction on Fe(III) (hydr)oxide reduction and microbial community development. *Geochim. Cosmochim. Acta* 129, 177–190.
- Lambertson, L., Nilsson, M., 2006. Organic material: the primary control on mercury methylation and ambient methyl mercury concentrations in estuarine sediments. *Environ. Sci. Technol.* 40, 1822–1829.
- Lazaro, W.L., Díez, S., da Silva, C.J., Ignácio, A.R., Guimarães, J.R., 2016. Waterscape determinants of net mercury methylation in a tropical wetland. *Environ. Res.* 150, 438–445.
- Lázaro, W.L., Díez, S., da Silva, C.J., Ignácio, Á.R.A., Guimarães, J.R.D., 2016. Waterscape determinants of net mercury methylation in a tropical wetland. *Environ. Res.* 150, 438–445.
- Leclercq, M., Planas, D., Amyot, M., 2015. Relationship between extracellular low-molecular-weight thiols and mercury species in natural lake periphytic biofilms. *Environ. Sci. Technol.* 49, 7709–7716.
- Leopold, K., Foulkes, M., Worsfold, P., 2010. Methods for the determination and speciation of mercury in natural waters—a review. *Anal. Chim. Acta* 663, 127–138.
- Li, P., Hur, J., 2017. Utilization of UV–vis spectroscopy and related data analyses for dissolved organic matter (DOM) studies: a review. *Crit. Rev. Environ. Sci. Technol.* 47, 131–154.
- Li, Y.-L., Vali, H., Yang, J., Phelps, T.J., Zhang, C.L., 2006. Reduction of iron oxides enhanced by a sulfate-reducing bacterium and biogenic H₂S. *Geomicrobiol. J.* 23, 103–117.
- Liem-Nguyen, V., 2016. Determination of Mercury Chemical Speciation in the Presence of Low Molecular Mass Thiols and Its Importance for Mercury Methylation. Department of Chemistry. Umeå University, Umeå.
- Lin, T.Y., Kampalath, R.A., Lin, C.C., Zhang, M., Chavarria, K., Lacson, J., Jay, J.A., 2013. Investigation of mercury methylation pathways in biofilm versus planktonic cultures of *Desulfovibrio desulfuricans*. *Environ. Sci. Technol.* 47, 5695–5702.
- Lindsay, M.B.J., Moncur, M.C., Bain, J.G., Jambor, J.L., Ptacek, C.J., Blowes, D.W., 2015. Geochemical and mineralogical aspects of sulfide mine tailings. *Appl. Geochem.* 57, 157–177.
- Liu, J., Valsaraj, K.T., Devai, I., DeLaune, R.D., 2008. Immobilization of aqueous Hg(II) by mackinawite (FeS). *J. Hazard. Mater.* 157, 432–440.
- Liu, P., Ptacek, C.J., Blowes, D.W., Bert, W.R., Landis, R.C., 2015. Aqueous leaching of organic acids and dissolved organic carbon from various biochars prepared at different temperatures. *J. Environ. Qual.* 44, 684–695.
- Liu, P., Ptacek, C.J., Blowes, D.W., Landis, R.C., 2016. Mechanisms of mercury removal by biochars produced from different feedstocks determined using X-ray absorption spectroscopy. *J. Hazard. Mater.* 308, 233–242.
- Liu, P., Ptacek, C.J., Elena, K.M.A., Blowes, D.W., Gould, W.D., Finck, Y.Z., Wang, A.O., Landis, R.C., 2018. Evaluation of mercury stabilization mechanisms by sulfurized biochars determined using X-ray absorption spectroscopy. *J. Hazard. Mater.* 347, 114–122.
- Lohmayer, R., Kappler, A., Lösekann-Behrens, T., Planer-Friedrich, B., 2014. Sulfur species as redox partners and electron shuttles for ferrihydrite reduction by *Sulfurospirillum deleyianum*. *Appl. Environ. Microbiol.* 80, 3141–3149.
- Lusila-Makiese, J.G., Tessier, E., Amouroux, D., Tutu, H., Chimuka, L., Weiersbye, I., Cukrowska, E.M., 2016. Mercury speciation and dispersion from an active gold mine at the West Wits area, South Africa. *Environ. Monit. Assess.* 188, 47.
- Mao, Y., Yin, Y., Li, Y., Liu, G., Feng, X., Jiang, G., Cai, Y., 2010. Occurrence of monomethylmercury in the Florida everglades: identification and verification. *Environ. Pollut.* 158, 3378–3384.
- Marvin-DiPasquale, M., Windham-Myers, L., Agee, J.L., Kakouros, E., Kieu le, H., Fleck, J.A., Alpers, C.N., Stricker, C.A., 2014. Methylmercury production in sediment from agricultural and non-agricultural wetlands in the Yolo Bypass, California, USA. *Sci. Total Environ.* 484, 288–299.
- Miao, Z., Brusseau, M.L., Carroll, K.C., Carreon-Diazconti, C., Johnson, B., 2012. Sulfate reduction in groundwater: characterization and applications for remediation. *Environ. Geochem. Health* 34, 539–550.
- Moreau, J.W., Gionfriddo, C.M., Krabbenhoft, D.P., Ogorek, J.M., DeWild, J.F., Aiken, G.R., Roden, E.E., 2015. The effect of natural organic matter on mercury methylation by *Desulfovibrio propionicus* 1p3r. *Front. Microbiol.* 6, 1389.
- Muyzer, G., Stams, A.J., 2008. The ecology and biotechnology of sulphate-reducing bacteria. *Nat. Rev. Microbiol.* 6, 441–454.
- Niu, Y., Qu, R., Liu, X., Mu, L., Bu, B., Sun, Y., Chen, H., Meng, Y., Meng, L., Cheng, L., 2014. Thiol-functionalized polysilsesquioxane as efficient adsorbent for adsorption of Hg(II) and Mn(II) from aqueous solution. *Mater. Res. Bull.* 52, 134–142.
- Park, J.-H., Wang, J.J., Zhou, B., Mikhael, J.E.R., DeLaune, R.D., 2019. Removing mercury from aqueous solution using sulfurized biochar and associated mechanisms. *Environ. Pollut.* 244, 627–635.
- Parkes, R.J., Dowling, N.J.E., White, D.C., Herbert, R.A., Gibson, G.R., 1993. Characterization of sulphate-reducing bacterial populations within marine and estuarine sediments with different rates of sulphate reduction. *FEMS Microbiol. Lett.* 102, 235–250.
- Parks, J.M., Johs, A., Podar, M., Bridou, R., Hurt, R.A., Smith, S.D., Tomanicek, S.J., Qian, Y., Brown, S.D., Brandt, C.C., Palumbo, A.V., Smith, J.C., Wall, J.D., Elias, D.A., Liang, L., 2013. The genetic basis for bacterial mercury methylation. *Science* 339, 1332–1335.
- Pelcová, P., Margetinová, J., Vaculovič, T., Komárek, J., Kubáň, V., 2010. Adsorption of mercury species on river sediments — effects of selected abiotic parameters. *Open Chemistry* 8.
- Poole, L.B., 2015. The basics of thiols and cysteines in redox biology and chemistry. *Free Radic. Biol. Med.* 80, 148–157.
- Poulin, B.A., Ryan, J.N., Aiken, G.R., 2014. Effects of iron on optical properties of dissolved organic matter. *Environ. Sci. Technol.* 48, 10098–10106.
- Praharaj, T., Fortin, D., 2008. Seasonal variations of microbial sulfate and iron reduction in alkaline Pb–Zn mine tailings (Ontario, Canada). *Appl. Geochem.* 23, 3728–3740.
- Pushie, M.J., Pickering, I.J., Korbas, M., Hackett, M.J., George, G.N., 2014. Elemental and chemically specific X-ray fluorescence imaging of biological systems. *Chem. Rev.* 114, 8499–8541.
- Qi, F., Kuppusamy, S., Naidu, R., Bolan, N.S., Ok, Y.S., Lamb, D., Li, Y., Yu, L., Semple, K.T., Wang, H., 2017. Pyrogenic carbon and its role in contaminant immobilization in soils. *Crit. Rev. Environ. Sci. Technol.* 47, 795–876.
- Randall, P.M., Yates, B.J., Lal, V., Darlington, R., Fimmen, R., 2013. In-situ subaqueous capping of mercury-contaminated sediments in a fresh-water aquatic system, part II—evaluation of sorption materials. *Environ. Res.* 125, 41–51.
- Ravichandran, M., 2004. Interactions between mercury and dissolved organic matter—a review. *Chemosphere* 55, 319–331.
- Ravichandran, M., Aiken, G.R., Reddy, M.M., Ryan, J.N., 1998. Enhanced dissolution of cinnabar (mercuric sulfide) by dissolved organic matter isolated from the Florida everglades. *Environ. Sci. Technol.* 32, 3305–3311.
- Reddy, K.R., DeLaune, R.D., 2008. Biogeochemical Characteristics. *Biogeochemistry of Wetlands*. CRC Press, pp. 27–65.
- Remy, S., Prudent, P., Probst, J.-L., 2006. Mercury speciation in soils of the industrialised Thur River catchment (Alsace, France). *Appl. Geochem.* 21, 1855–1867.
- Roden, E.E., 2003. Fe(III) oxide reactivity toward biological versus chemical reduction. *Environ. Sci. Technol.* 37, 1319–1324.
- Roulet, M., Guimarães, J.-R.D., Lucotte, M., 2001. Methylmercury production and accumulation in sediments and soils of an Amazonian floodplain — effect of seasonal inundation. *Water Air Soil Pollut.* 128, 41–60.
- Rubino, F.M., 2015. Toxicity of glutathione-binding metals: a review of targets and mechanisms. *Toxics* 3, 20–62.
- Rytuba, J.J., 2000. Mercury mine drainage and processes that control its environmental impact. *Sci. Total Environ.* 260, 57–71.
- Sarkar, D., Essington, M.E., Misra, K.C., 1999. Adsorption of mercury(II) by variable charge surfaces of quartz and gibbsite contribution from the Dep. of Plant and Soil Sciences, The Univ. of Tennessee. *Soil Sci. Soc. Am. J.* 63, 1626–1636.
- Schenk, R., 1994. Verteilung und Dynamik von Schwermetallen in Sedimenten der Wupper. Heinrich-Heine Universität, Düsseldorf.
- Shao, D., Kang, Y., Wu, S., Wong, M.H., 2012. Effects of sulfate reducing bacteria and sulfate concentrations on mercury methylation in freshwater sediments. *Sci. Total Environ.* 424, 331–336.
- Shen, B., Tian, L., Li, F., Zhang, X., Xu, H., Singh, S., 2017. Elemental mercury removal by the modified bio-char from waste tea. *Fuel* 187, 189–196.
- Shu, R., Dang, F., Zhong, H., 2016a. Effects of incorporating differently-treated rice straw on phytoavailability of methylmercury in soil. *Chemosphere* 145, 457–463.
- Shu, R., Wang, Y., Zhong, H., 2016b. Biochar amendment reduced methylmercury accumulation in rice plants. *J. Hazard. Mater.* 313, 1–8.
- Šípková, A., Száková, J., Hanč, A., Tlustoš, P., 2016. Mobility of mercury in soil as affected by soil physicochemical properties. *J. Soils Sediments* 16, 2234–2241.
- Skylberg, U., 2010. Chapter 13 - mercury biogeochemistry in soils and sediments. In: Balwant, S., Markus, G. (Eds.), *Developments in Soil Science*. Elsevier.
- Skylberg, U., 2012. Chemical Speciation of Mercury in Soil and Sediment. *Environmental Chemistry and Toxicology of Mercury*. John Wiley Sons, Inc.
- Song, X., Ye, M., Tang, X., Wang, C., 2013. Ionic liquids dispersive liquid-liquid micro-extraction and HPLC-atomic fluorescence spectrometric determination of mercury species in environmental waters. *J. Sep. Sci.* 36, 414–420.
- Song, Y., Jiang, T., Liem-Nguyen, V., Sparrman, T., Björn, E., Skylberg, U., 2018. Thermodynamics of Hg(II) bonding to thiol groups in Suwannee River natural organic matter resolved by competitive ligand exchange, Hg LIII-edge EXAFS and (1)H NMR spectroscopy. *Environ. Sci. Technol.* 52, 8292–8301.
- Strickman, R.J., Mitchell, C.P.J., 2018. Mercury methylation in stormwater retention ponds at different stages in the management lifecycle. *Environ. Sci. Processes Impacts* 20, 595–606.
- Sunderland, E.M., Gobas, F.A.P.C., Branfireun, B.A., Heyes, A., 2006. Environmental controls on the speciation and distribution of mercury in coastal sediments. *Mar.*

- Chem. 102, 111–123.
- Takeo, N., 2005. Atlas of eh-pH diagrams. Intercomparison of thermodynamic databases. In: Technology, N.I.o.A.I.S.a. (Ed.), Geological Survey of Japan.
- Tan, Z., Qiu, J., Zeng, H., Liu, H., Xiang, J., 2011. Removal of elemental mercury by bamboo charcoal impregnated with H₂O₂. *Fuel* 90, 1471–1475.
- Taube, F., Pommer, L., Larsson, T., Shchukarev, A., Nordin, A., 2008. Soil remediation – mercury speciation in soil and vapor phase during thermal treatment. *Water Air Soil Pollut.* 193, 155–163.
- Tipping, E., Lofts, S., Hooper, H., Frey, B., Spurgeon, D., Svendsen, C., 2010. Critical limits for Hg(II) in soils, derived from chronic toxicity data. *Environ. Pollut.* 158, 2465–2471.
- Tsui, M.T., Finlay, J.C., 2011. Influence of dissolved organic carbon on methylmercury bioavailability across Minnesota stream ecosystems. *Environ. Sci. Technol.* 45, 5981–5987.
- U.S. EPA Method 3051A, 2007. Method 3051A. Microwave Assisted Acid Digestion of Sediments, Sludges, Soils, and Oils.
- Ullah, A., Heng, S., Munis, M.F.H., Fahad, S., Yang, X., 2015. Phytoremediation of heavy metals assisted by plant growth promoting (PGP) bacteria: a review. *Environ. Exp. Bot.* 117, 28–40.
- Ullrich, S.M., Tanton, T.W., Abdrashitova, S.A., 2001. Mercury in the aquatic environment: a review of factors affecting methylation. *Crit. Rev. Environ. Sci. Technol.* 31, 241–293.
- Wallschläger, D., Desai, M.V.M., Wilken, R.-D., 1996. The role of humic substances in the aqueous mobilization of mercury from contaminated floodplain soils. *Water Air Soil Pollut.* 90, 507–520.
- Wang, J., Feng, X., Anderson, C.W.N., Wang, H., Wang, L., 2013. Thiosulphate-induced mercury accumulation by plants: metal uptake and transformation of mercury fractionation in soil - results from a field study. *Plant Soil* 375, 21–33.
- Weishaar, J.L., Aiken, G.R., Bergamaschi, B.A., Fram, M.S., Fujii, R., Mopper, K., 2003. Evaluation of specific ultraviolet absorbance as an indicator of the chemical composition and reactivity of dissolved organic carbon. *Environ. Sci. Technol.* 37, 4702–4708.
- White, D.C., Davis, W.M., Nickels, J.S., King, J.D., Bobbie, R.J., 1979. Determination of the sedimentary microbial biomass by extractable lipid phosphate. *Oecologia* 40, 51–62.
- White, D., Stair, J., Ringelberg, D., 1996. Quantitative comparisons of in situ microbial biodiversity by signature biomarker analysis. *J. Ind. Microbiol.* 17, 185–196.
- Windham-Myers, L., Marvin-Dipasquale, M., Krabbenhoft, D.P., Agee, J.L., Cox, M.H., Heredia-Middleton, P., Coates, C., Kakouros, E., 2009. Experimental removal of wetland emergent vegetation leads to decreased methylmercury production in surface sediment. *J. Geophys. Res.* 114.
- Wouters, M.A., Fan, S.W., Haworth, N.L., 2010. Disulfides as redox switches: from molecular mechanisms to functional significance. *Antioxid. Redox Signal.* 12, 53–91.
- Xia, K., Skyllberg, U.L., Bleam, W.F., Bloom, P.R., Nater, E.A., Helmke, P.A., 1999. X-ray absorption spectroscopic evidence for the complexation of Hg(II) by reduced sulfur in soil humic substances. *Environ. Sci. Technol.* 33, 257–261.
- Xia, S., Huang, Y., Tang, J., Wang, L., 2019. Preparation of various thiol-functionalized carbon-based materials for enhanced removal of mercury from aqueous solution. *Environ. Sci. Pollut. Res.* <https://doi.org/10.1007/s11356-019-04320-0>.
- Xu, J., Kleja, D.B., Biester, H., Lagerkvist, A., Kumpiene, J., 2014. Influence of particle size distribution, organic carbon, pH and chlorides on washing of mercury contaminated soil. *Chemosphere* 109, 99–105.
- Xu, J., Bravo, A.G., Lagerkvist, A., Bertilsson, S., Sjoblom, R., Kumpiene, J., 2015. Sources and remediation techniques for mercury contaminated soil. *Environ. Int.* 42–53 74C.
- Xu, X., Schierz, A., Xu, N., Cao, X., 2016. Comparison of the characteristics and mechanisms of Hg(II) sorption by biochars and activated carbon. *J. Colloid Interface Sci.* 463, 55–60.
- Yang, J., Zhao, Y., Ma, S., Zhu, B., Zhang, J., Zheng, C., 2016. Mercury removal by magnetic biochar derived from simultaneous activation and magnetization of sawdust. *Environ. Sci. Technol.* 50, 12040–12047.
- Yin, Y., Allen, H.E., Li, Y., Huang, C.P., Sanders, P.F., 1996. Adsorption of mercury(II) by soil: effects of pH, chloride, and organic matter. *J. Environ. Qual.* 25, 837–844.
- Yoon, S.-J., Diener, L.M., Bloom, P.R., Nater, E.A., Bleam, W.F., 2005. X-ray absorption studies of CH₃Hg⁺ -binding sites in humic substances. *Geochim. Cosmochim. Acta* 69, 1111–1121.
- Yu, K., Rinklebe, J., 2011. Advancement in soil microcosm apparatus for biogeochemical research. *Ecol. Eng.* 37, 2071–2075.
- Yu, K., Böhme, F., Rinklebe, J., Neue, H.-U., DeLaune, R.D., 2007. Major biogeochemical processes in soils-a microcosm incubation from reducing to oxidizing conditions. *Soil Sci. Soc. Am. J.* 71, 1406.
- Zhang, S., Yang, X., Ju, M., Liu, L., Zheng, K., 2019. Mercury adsorption to aged biochar and its management in China. *Environ. Sci. Pollut. Res.* 26, 4867–4877.
- Zhu, H., Zhong, H., Evans, D., Hintelmann, H., 2015. Effects of rice residue incorporation on the speciation, potential bioavailability and risk of mercury in a contaminated paddy soil. *J. Hazard. Mater.* 293, 64–71.